Systems Biology of Tomato Fruit Development: Combined Transcript, Protein, and Metabolite Analysis of Tomato Transcription Factor (*nor, rin*) and Ethylene Receptor (*Nr*) Mutants Reveals Novel Regulatory Interactions[1][W][OA]

Sonia Osorio[2], Rob Alba[2,3], Cynthia M.B. Damasceno[4], Gloria Lopez-Casado, Marc Lohse, Maria Inés Zanor[5], Takayuki Tohge, Björn Usadel, Jocelyn K.C. Rose, Zhangjun Fei, James J. Giovannoni, and Alisdair R. Fernie*

Max-Planck-Institut für Molekulare Pflanzenphysiologie, 14476 Potsdam-Golm, Germany (S.O., M.L., M.I.Z., T.T., B.U., A.R.F.); and Boyce Thompson Institute for Plant Research and United States Department of Agriculture-Agricultural Research Service Robert W. Holley Center (R.A., Z.F., J.J.G.) and Department of Plant Biology (C.M.B.D., G.L.-C., J.K.C.R.), Cornell University, Ithaca, New York 14853

Tomato (*Solanum lycopersicum*) is an established model to study fleshy fruit development and ripening. Tomato ripening is regulated independently and cooperatively by ethylene and transcription factors, including nonripening (*NOR*) and ripening-inhibitor (*RIN*). Mutations of *NOR*, *RIN*, and the ethylene receptor *Never-ripe* (*Nr*), which block ethylene perception and inhibit ripening, have proven to be great tools for advancing our understanding of the developmental programs regulating ripening. In this study, we present systems analysis of *nor, rin*, and *Nr* at the transcriptomic, proteomic, and metabolomic levels during development and ripening. Metabolic profiling marked shifts in the abundance of metabolites of primary metabolism, which lead to decreases in metabolic activity during ripening. When combined with transcriptomic and proteomic data, several aspects of the regulation of metabolism during ripening were revealed. First, correlations between the expression levels of a transcript and the abundance of its corresponding protein were infrequently observed during early ripening, suggesting that posttranscriptional regulatory mechanisms play an important role in these stages; however, this correlation was much greater in later stages. Second, we observed very strong correlation between ripening-associated transcripts and specific metabolite groups, such as organic acids, sugars, and cell wall-related metabolites, underlining the importance of these metabolic pathways during fruit ripening. These results further revealed multiple ethylene-associated events during tomato ripening, providing new insights into the molecular biology of ethylene-mediated ripening regulatory networks.

Fruit ripening is a complex developmental program involving the coordinated regulation of numerous metabolic pathways that influence color, flavor, aroma, and texture. Many of these attributes enhance fruit nutritional value and attractiveness, thereby promoting consumption and seed dispersal (Liu et al., 2004; Goff and Klee, 2006) by offering important dietary minerals, vitamins, fibers, and antioxidants to seed-dispersing organisms.

Insights into the genetic mechanisms that mediate fruit ripening-related processes, such as cell wall metabolism, pigment synthesis, and sugar metabolism, have resulted from studies that collectively span a wide range of plant species and indicate that they are broadly conserved (Seymour, 1993; Carrari and Fernie, 2006; Fait et al., 2008; Moing et al., 2011; Zhang et al., 2011). However, tomato (*Solanum lycopersicum*) has emerged as the primary experimental model in which to study the development and ripening of fleshy fruits (Giovannoni, 2004; Fernandez et al., 2009). This reflects its economic importance and many favorable genetic characteristics, such as small genome size (950 Mb), a relatively short life cycle, and routine transient and stable genetic transformation.

The many studies of the development and maturation of tomato fruits have resulted in the identification

[1] This work was supported by the National Science Foundation (grant no. DBI–0606595 to J.K.C.R. and grant no. DBI–0923312 J.J.G.).

[2] These authors contributed equally to the article.

[3] Present address: Composition and Nutrition Team, Monsanto Company, St. Louis, MO 63167.

[4] Present address: Embrapa Maize and Sorghum, Sete Lagoas, 35702–098 Brazil.

[5] Present address: Instituto de Biología Molecular y Celular de Rosario (IBR-CONICET), Facultad de Ciencias Bioquímicas y Farmacéuticas (UNR) Suipacha 530, Rosario S2002LRK, Argentina.

* Corresponding author; e-mail fernie@mpimp-golm.mpg.de.

The author responsible for distribution of materials integral to the findings presented in this article in accordance with the policy described in the Instructions for Authors (www.plantphysiol.org) is: Alisdair R. Fernie (fernie@mpimp-golm.mpg.de).

[W] The online version of this article contains Web-only data.

[OA] Open Access articles can be viewed online without a subscription.

www.plantphysiol.org/cgi/doi/10.1104/pp.111.175463

of specific genes that participate in ripening (Vrebalov et al., 2002; Manning et al., 2006; Wang et al., 2009; Chung et al., 2010; Nashilevitz et al., 2010; Karlova et al., 2011; for review, see Giovannoni, 2007; Matas et al., 2009). Similarly, much has been learned about the substantial changes in both primary and secondary metabolism that accompany tomato fruit ripening, although much of these data have not been directly related to regulatory events (Carrari and Fernie, 2006) and often target specific pathways. On a more comprehensive scale, tomato development has also been examined at the levels of transcriptome (Alba et al., 2005; Lemaire-Chamley et al., 2005; Carrari et al., 2006; Vriezen et al., 2008; Wang et al., 2009), proteome (Saravanan and Rose, 2004; Faurobert et al., 2007; Page et al., 2010), and metabolome (Roessner-Tunali et al., 2003; Carrari et al., 2006; Fraser et al., 2007; Moco et al., 2007) characterization. However, to date, relatively few analyses have combined multilevel approaches (Carrari et al., 2006; Armengaud et al., 2009; Enfissi et al., 2010; Zamboni et al., 2010), and those that have are limited with respect to genotype, developmental stage, or the number of parameters measured.

A number of important advances in our understanding of the mechanisms that regulate ripening have also come from the characterization of monogenic tomato mutants, including *ripening-inhibitor* (*rin*), *nonripening* (*nor*), *colorless nonripening* (*Cnr*), *green-ripe* (*Gr*), *green flesh* (*gf*), *high pigment1* (*hp1*), *high pigment2* (*hp2*), and *never-ripe* (*Nr*; Lanahan et al., 1994; Mustilli et al., 1999; Vrebalov et al., 2002; Liu et al., 2004; Barry and Giovannoni, 2006; Manning et al., 2006; Barry et al., 2008). Although the complete network of ripening regulatory pathways remains to be resolved, cloning of many of the underlying genes has provided insights into their respective roles and hierarchical relationships (Giovannoni, 2004). The *rin* and *Cnr* loci encode a MADS box and a SPBP transcription factor, respectively, and are necessary regulators of ripening (Vrebalov et al., 2002; Manning et al., 2006). The *Gr* gene is suggested to interact with components of the fruit-specific ethylene response (Barry and Giovannoni, 2006), while the *Nr* mutation has been characterized as an ERS-like ethylene receptor that is impaired in the ability to bind ethylene (Lanahan et al., 1994). The high-pigment mutations influence the role of light in ripe fruit pigmentation via tomato orthologs of the *DEETIOLATED* and *DAMAGED DNA-BINDING PROTEINS1*, genes originally defined in Arabidopsis (*Arabidopsis thaliana*; Mustilli et al., 1999; Liu et al., 2004). The *gf* gene encodes a senescence-associated STAY-GREEN protein, indicating a role for plastids in both manifesting and regulating ripening phenotypes (Barry et al., 2008).

The identification and characterization of such mutants provide an opportunity to dissect the complex networks of ripening-related pathways at multiple levels. In this study, we have examined three dominant ripening mutants of tomato, *nor*, *rin*, and *Nr*, along the developmental and ripening periods at the transcriptomic, proteomic, and metabolomic levels in order to further extend the analysis carried out by Alba et al. (2005). Use of these specific mutants helps define transcriptional activity as transcriptionally regulated and ethylene response subtranscriptomes. Transcriptional analysis was carried out using the tomato cDNA microarray (TOM1; Alba et al., 2005), microarray-containing ESTs, proteomic data were obtained using isobaric tag labeling (iTRAQ; Wise et al., 2007), and metabolomics data were obtained by gas chromatography-mass spectrometry (GC-MS) according to Carrari et al. (2006). The combined results are discussed in the context of current models of ripening and development.

RESULTS

Experimental Design

The experiments described here were designed to span tomato fruit ripening in cv Ailsa Craig, which occurred under greenhouse conditions over a period of 57 d from fruit set to a fully ripe stage. Tomato fruit development can be divided into four major phases: cell differentiation, division, expansion, and ripening (Gillaspy et al., 1993). As described by Alba et al. (2005), these phases correspond to wild-type fruits between 7 and 27 d after pollination (DAP) for the first two phases, to the first visible carotenoid accumulation (42 DAP) in the third phase, and to full red color development (57 DAP) in the ripening phase. Pericarp of anthesis-tagged and equivalent age fruits of the *rin*, *nor*, and *Nr* isogenic mutants was harvested (one biological replicate was considered an individual fruit from different plants). We note that at stages following mature green (39 DAP), the mutant fruits diverge in their development from the wild type, as they are indeed substantially (*Nr*) or nearly completely (*rin* and *nor*) ripening inhibited. Changes resulting from the selected mutations may result in delayed effects, which could be further compounded by occurring in the context of an older fruit, where developmental context is altered due to the normal progression of activities not impacted by the mutations employed. Thus, while an alternative to comparing identically aged fruit would be to compare identical physiological stages such as breaker or red ripe, *rin* and *nor* never achieve comparable stages and *Nr* in the Ailsa Craig background does not achieve red ripe (and breaker is delayed). We have thus selected comparison of identically staged fruits, as this approach allows for comparison of changes in the context of a developmental parameter (age post pollination) that can be measured accurately in all genotypes.

Subsequently, transcriptome analysis was carried out using two-color hybridizations of the TOM1 array, which contains 12,899 different EST clones representing approximately 8,500 tomato genes, using mRNA prepared from each stage. Proteomic data from three

ripening stages (39, 42, and 52 DAP) were obtained using the iTRAQ labeling technique. A total of 48 primary metabolites were analyzed by GC-time of flight-MS in fruits harvested between 27 and 57 DAP for *nor* and *rin* and from 42 to 57 DAP for *Nr*, as described in "Materials and Methods."

Transcriptomic Profiling

We investigated differential transcript accumulation using two-color simultaneous hybridizations of the TOM1 array during tomato development for the wild type, *Nr*, *nor*, and *rin* (10 time points: 7, 17, 27, 39, 41, 42, 43, 47, 52, and 57 DAP). The transcript data for *Nr* has previously been published (Alba et al., 2005); however, it is included here for comparative purposes and in the broader context of the orthogonal data sets. It is important to note in interpreting our results that *Nr* in the Ailsa Craig background retains partial ethylene sensitivity and thus partial ripening occurs (Yen et al., 1995).

The PageMan (Usadel et al., 2006) and MapMan (Usadel et al., 2005) mapping files, described in "Materials and Methods," were used to study the development and ripening of *Nr*, *nor*, and *rin* by identifying significantly overrepresented functional groups, in comparison with the corresponding wild-type control samples, on the basis of Fisher's exact tests and Wilcoxon tests for each category. This facilitated the analysis of the global activation and/or repression of metabolic pathways and gene regulatory networks of the pericarp. We identified metabolic pathways that were enriched during these processes, including several that would be anticipated based on previous studies, including hormone metabolism (Supplemental Fig. S1). The individual gene responses can be viewed in MapMan (Supplemental Data Set S1; Supplemental File S1).

Visual inspection revealed the categories with either qualitatively similar or different responses between the mutants and the control. The general down-regulation of photosynthetic light reactions during the studied stages of *Nr* is immediately apparent, suggestive of reduced photosynthesis and reduced carbon assimilation in the fruit. In addition, this mutant is characterized by an induction of genes associated with the Suc-to-starch transition, being most prominent at 42 DAP for genes related to Suc degradation and at 17 DAP onward for genes associated with starch synthesis. In *rin*, transcripts related to starch synthesis appear to exhibit a biphasic response, with a large induction occurring relatively early followed by a secondary increase (43 and 52 DAP). Moreover, these transcripts appear to be up-regulated in *nor* at 27 and 41 DAP (Supplemental Fig. S1). These results point to the importance of hexoses derived from the degradation of Suc for starch synthesis during early tomato development and at the onset of ripening and are consistent with a recent study highlighting the importance of transitory starch in normal fruit development (Centeno et al., 2011).

A spectrum of genes/proteins involved in cell wall restructuring and disassembly (such as endo-β-1, 4-glucanases from the glycosyl hydrolase [GH] family, expansins, xyloglucan transglucosylase hydrolases [GH16], and a range of pectinases) are canonically associated with fruit development and ripening (Rose and Bennett, 1999; Rose et al., 2004b; Brummell, 2006). In our study, a number of genes associated with cell wall degradation were down-regulated during ripening in *nor* and *rin*, while those putatively involved in reversible wall loosening and assembly were down-regulated at 27 and 41 DAP in *Nr*, consistent with the previously observed depolymerization of cell wall components at the onset of storage mobilization (Amor et al., 1995; Reiter, 2008; Supplemental Fig. S1). At the onset of ripening (42 DAP), genes associated with amino acid synthesis were expressed at higher levels, including the Asp-derived Met pathway in *nor*, *rin*, and *Nr* (Supplemental Fig. S1). In contrast, we could infer that amino acid degradation metabolism is generally repressed in all three mutants, and the phytoene synthase-1 gene is down-regulated at the 42-DAP stage (breaker) in *nor* and at 47 DAP in *rin* but 1 d before breaker (41 DAP) for *Nr* (Supplemental Fig. S1).

The expression of genes associated with hormone biosynthetic pathways was altered in *Nr* and *rin*, consistent with the lack of climacteric ethylene production and activity in these nonripening fruits. During ripening, transcripts for genes involved in the biosynthesis of ethylene were expressed at high levels in *Nr* as well as observed in *rin*, but almost no change was observed in the same time frame for *nor*, suggesting that *nor* activity my be upstream of *rin* in the regulatory hierarchy. Besides the well-characterized participation of ethylene in the control of ripening in climacteric fruits (Giovannoni, 2004, 2007; Alba et al., 2005), other hormones have more recently been demonstrated to play important roles (Martí et al., 2007; Chaabouni et al., 2009; Yang et al., 2010). These data indicate that a highly complex interactive hormonal network likely regulates fruit ripening. In *Nr*, transcripts for genes involved in the biosynthesis of auxin and jasmonate were up-regulated at 42 DAP (breaker stage) and 52 DAP, respectively, while *nor* was characterized by a down-regulation of abscisic acid metabolism at the end of ripening (57 DAP; Supplemental Fig. S1). Interestingly, transcripts associated with ethylene perception and signal transduction changed relatively little but were significantly down-regulated during ripening in *nor* (Supplemental File S1; Supplemental Fig. S1).

We additionally observed differential expression of transcripts involved in protein synthesis, which were down-regulated during all ripening phases in *Nr* but were up-regulated during earlier development in *nor* and also during the period that would correspond to normal ripening in *rin*. Moreover, genes involved in protein degradation were up-regulated in *Nr* (Supplemental Fig. S1).

While the changes described above suggest considerable alterations in the programs influencing early development and ripening in the mutants, a linear analysis on a time point-by-time point basis may exaggerate the differences between the genotypes. Therefore, we reanalyzed the data such that gene expression at any time point was compared, within genotypes only, with the first harvested time point (Fig. 1; Supplemental Fig. S2; Supplemental Table S1). These data revealed a general down-regulation of photosynthetic light reactions during development and ripening in the wild type and the *rin* mutant (Fig. 1) and similarly in *nor* and *Nr*, but only from 39 DAP onward. In addition, the *Nr* mutant showed up-regulation of these genes in the first two developmental stages (17 and 27 DAP; Fig. 1). The Calvin-Benson cycle was apparently down-regulated at the 39- and 41-DAP stages during normal tomato fruit development (Fig. 1A) but across all studied stages in *rin* (Fig. 1C). A similar pattern of changes was observed from the 39-DAP stage in *Nr*, which also showed up-regulation in the two earliest stages (17 and 27 DAP; Fig. 1C). The same down-regulation was observed for *nor* at later stages (43, 47, and 57 DAP; Fig. 1B).

The transcript analysis suggested that starch synthesis was down-regulated from 17 DAP onward

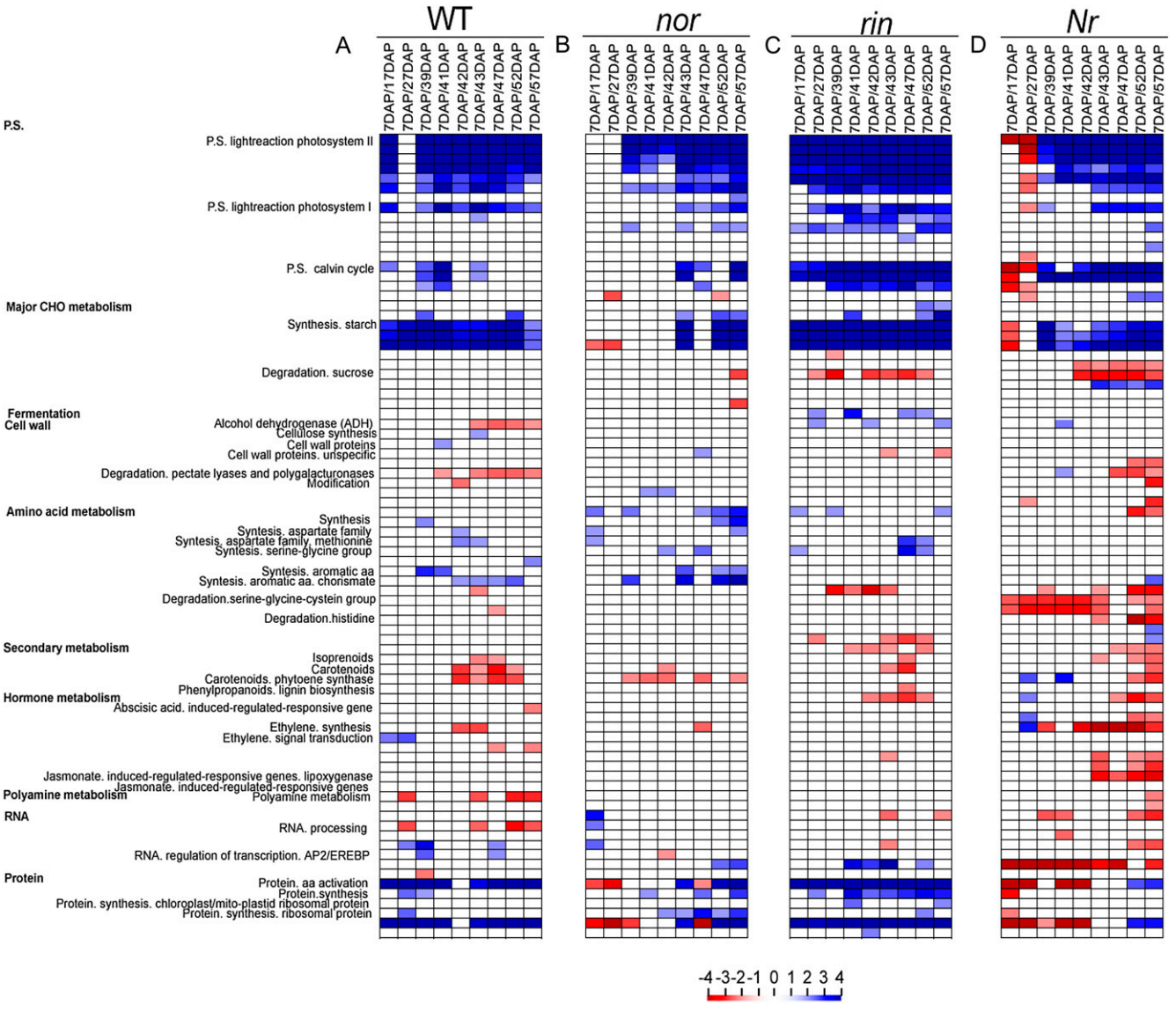

Figure 1. Expression analysis in the wild type (WT), *nor*, *rin*, and *Nr*. A condensed PageMap display of altered pathways is shown. Gene expression data are presented as $\log_2$ fold changes in comparison with the first harvested time point (7 DAP) within genotypes. The analyzed time points were 7, 17, 27, 39, 41, 42, 43, 47, 52, and 57 DAP. The data were subjected to a Wilcoxon test in PageMan, and the results are displayed in false-color code. Bins colored in red are significantly up-regulated, whereas bins colored in blue are significantly down-regulated. CHO, Carbohydrate.

during normal fruit development and ripening, with a similar pattern of changes seen in *rin* and *Nr*. However, in *Nr*, this trend was only significant from the 39-DAP stage onward (Fig. 1, C and D). On the other hand, *nor* only showed this behavior in later ripening stages (43, 52, and 57 DAP; Fig. 1B). Another process related to sugar metabolism, the degradation of Suc, was suggested to be up-regulated in all three mutants, but with differing temporal patterns: from 42 DAP (breaker) in *Nr*, 27 and 39 DAP in *rin*, but only in the last ripening stage (57 DAP) in *nor* (Fig. 1, B–D). Again, the more pronounced impact of *nor* on starch and Suc metabolism is consistent with an earlier or more global role in ripening for *nor* than *rin* or *Nr*.

Another well-characterized ripening-related process is the activation of alcohol hydrogenase (Carrari and Fernie, 2006). Analysis of the alcohol hydrogenase-associated transcripts suggested a similar pattern in *nor*, *rin*, and the wild type, but it only occurred at 43 DAP (Fig. 1B) in *nor*, at 39, 42, and 47 DAP in *rin* (Fig. 1C), and in all ripening stages in the wild type (Fig. 1A). We also observed that TCA metabolism was up-regulated across the later stages in *Nr* (43, 47, and 57 DAP) but down-regulated in *rin* and *nor* mutants at this time point (Fig. 1, B–D).

Genes associated with pectin degradation (pectate lyase and polygalacturonase) are clearly up-regulated during normal ripening in tomato fruit, as expected (Fig. 1A), but this pattern was delayed in *Nr*, consistent with the residual ethylene response and partial ripening (up-regulated in 47, 52, and 57 DAP; Fig. 1D), and not observed in the other two mutants (Fig. 1, B and C). Several genes related to reversible wall modification were up-regulated at the 42-DAP stage in the wild type, while *nor* showed no such changes. However, these genes were up-regulated at the 43- and 57-DAP stages in *rin* (Fig. 1C) but in *Nr* only at 57 DAP (Fig. 1D).

The transcript pattern suggested that synthesis of aromatic amino acids was down-regulated from 39 DAP onward in the wild type (Fig. 1A), while the associated genes showed the same behavior at later stages in the three mutants (Fig. 1, B–D): 43, 52, and 57 DAP in *nor*; 47 and 52 DAP in *rin*; and 57 DAP in *Nr*. Interestingly, Ser, Gly, and Cys degradation was up-regulated at the 47-DAP stage during fruit development in the wild type (Fig. 1A) and throughout all stages of development in *Nr*, but not in *rin* or *nor* (Fig. 1, B–D).

At the onset of ripening (42 DAP), transcripts associated with isoprenoid and carotenoid metabolism were up-regulated in normal ripening (Fig. 1A), whereas in both *nor* and *rin*, this was apparent at earlier stages (Fig. 1, B and C). In contrast, in *Nr*, this pattern was observed in later stages (52 and 57 DAP, again consistent with the partially ripening phenotype), exemplified by phytoene synthase-1, which was down-regulated in earlier development (27 and 41 DAP; Fig. 1D). As was expected from previous studies (Alba et al., 2005; Carrari and Fernie, 2006), ethylene metabolism was altered in all three mutants. In the wild-type fruit, we observed an induction of ethylene biosynthesis at 42 DAP (breaker stage), with a similar pattern of changes seen in *Nr* (Fig. 1, A and D). Additionally, in the first developmental stages (17 and 27 DAP), a down-regulation of genes related to ethylene signal transduction was apparent (Fig. 1A). In *rin*, the up-regulation was also displayed at the same stage as in the wild type (42 DAP) but subsequently continued throughout ripening until 52 DAP, as in *Nr* (Fig. 1C), but in *nor*, the induction of ethylene biosynthesis was delayed (Fig. 1B). In addition, the *Nr* mutant displayed an apparent up-regulation of jasmonate metabolism during the ripening process (from 43 to 57 DAP).

During development of wild-type tomato fruit, we observed a down-regulation of polyamine synthesis in the earlier stages (27 and 39 DAP) and also at a later stage (47 DAP; Fig. 1A), while *Nr* showed up-regulation late in development (57 DAP; Fig. 1D) and no significant changes were observed in *rin* and *nor* (Fig. 1, B and C).

A general up-regulation of transcription regulatory genes was observed at 27 DAP and also from 42 DAP (breaker stage) until 57 DAP during normal tomato fruit development (Fig. 1A). In *rin*, this up-regulation was only significant at 43 DAP, and the same behavior was observed in the *Nr* mutant, but again in later stages (52 and 57 DAP; Fig. 1D). However, in *nor*, the only obvious difference was a down-regulation at 17 DAP (Fig. 1B). Interestingly, the transcription factor family APETALA2 (AP2/EREBP), one member of which (*AP2a*) has been described as a ripening-related repressor of ethylene response (Chung et al., 2010), was substantially up-regulated in *nor* (Fig. 1B) at the time point equivalent to the onset of ripening in the wild type (42 DAP).

It is also worth noting that general down-regulation of genes involved in the biosynthesis of ribosomal proteins occurred in both the wild type and *rin* (Fig. 1, A and C). In *nor* and *Nr*, these genes showed the same patterns during ripening (43, 52, and 57 DAP for *nor* and 52 and 57 DAP for *Nr*). However, these genes were up-regulated in earlier stages (17, 27, and 39 DAP for *nor* and 17, 27, 39, 41, and 42 DAP for *Nr*; Fig. 1, B and D).

Metabolic Profiling

To follow the repertoire of metabolic changes that occur during tomato development in the three mutants, we carried out extensive metabolic profiling for primary metabolism using an established GC-MS method (Fernie et al., 2004). For the analysis, we selected several stages that span development and ripening for *nor* and *rin* (27, 39, 41, 42, 43, 47, 52, and 57 DAP) and from 42 DAP onward for *Nr*. Carrari et al. (2006) presented an exhaustive metabolic study of fruit development and ripening in the Moneymaker tomato cultivar, which shows similarities and also differences

in metabolite behavior compared with the cultivar used in this study (Ailsa Craig). In the previous study, it was reported that Suc decreased strongly during the first developmental stages, until 28 DAP, and in parallel Glc and Fru accumulated in an essentially linear manner. However, these changes were not observed in Ailsa Craig (Fig. 2; Supplemental Data Set S3). Instead, Suc levels decreased during the transition to ripening

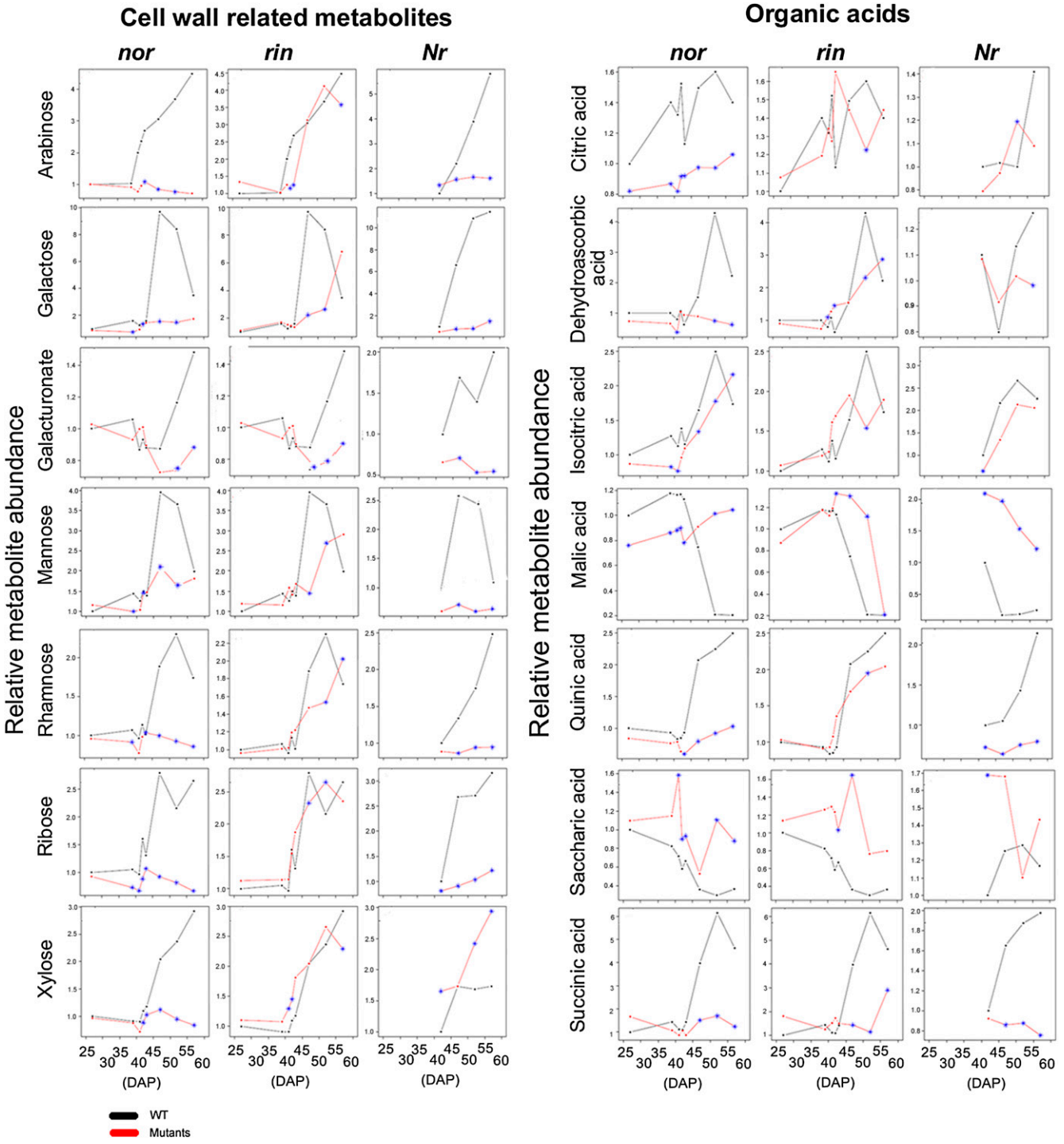

Figure 2. Primary metabolite levels in the wild type (WT), *nor*, *rin*, and *Nr*. Time points presented are 17, 27, 39, 41, 42, 43, 47, 52, and 57 DAP. Data are normalized to the mean response calculated for the wild type at 7 DAP. Values presented are means SE of five replicates. Asterisks Q28denote differences that were determined to be significant by Student's *t* test analysis ($P \leq 0.05$) compared with wild-type samples harvested at the same stage.

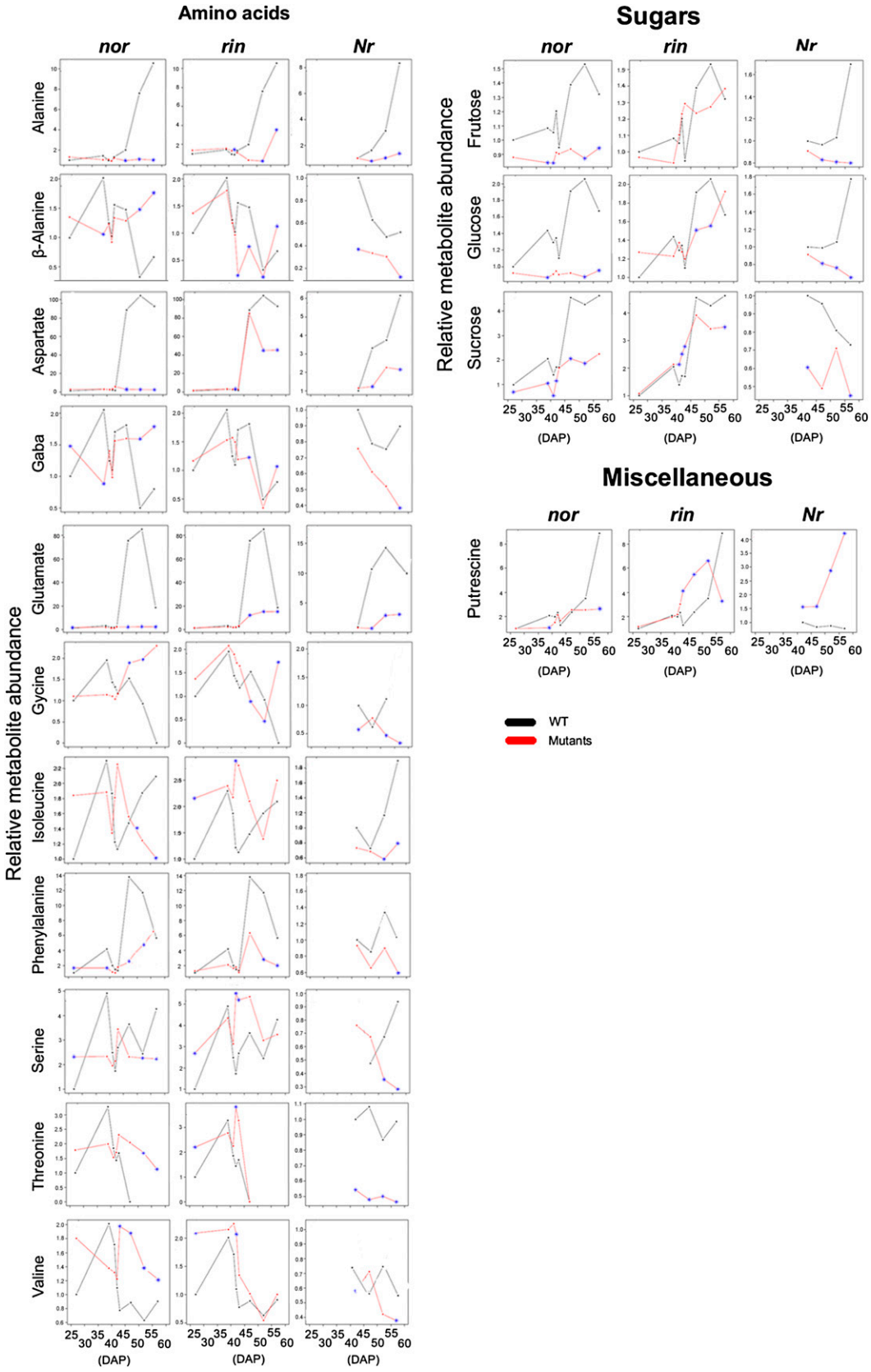

Figure 2. (*Continued.*)

(41, 42, and 43 DAP) and later increased (52 and 57 DAP). Glc and Fru also exhibited a reduction during the development-ripening transition (41 and 42 DAP) and increased in the same stages as Suc (Fig. 2). We observed that the levels of Glc, Fru, and Suc were reduced in the three mutants across the time course. Although starch degradation has not been subjected to detailed characterization in tomato pericarp tissue, it would thus appear that tomato fruit, like Arabidopsis leaves (Niittylä et al., 2004), are largely reliant on the hydrolytic pathway of degradation.

We were also able to detect the levels of a total of 11 amino acids across all genotypes. The three mutants and the wild type all revealed marked alterations during development and ripening (Fig. 2). Two main patterns of amino acid accumulation were apparent: (1) those increasing during ripening, and (2) those decreasing exclusively during ripening. Group 1 was dominated by Phe, Asp, Ile, Glu, and Ala, while group 2 consisted of γ-aminobutyrate (GABA), β-Ala, Thr, Ser, Gly, and Val. A comparison of these patterns with those observed by Carrari et al. (2006) in Moneymaker revealed that the two cultivars display strikingly similar shifts in amino acid levels. That said, a few cultivar-specific differences were apparent, such as a decrease in Ala during development in Moneymaker (Carrari et al., 2006) but not in Ailsa Craig (Fig. 2). Interestingly, when comparing the metabolic shifts displayed by the mutants, we observed that in all three mutants, Asp, Glu, and Ala, which were characterized by increases on ripening in the wild type, were slightly increased or unaltered during earlier development and ripening (Fig. 2). Moreover, during ripening, *nor* accumulated considerable amounts of β-Ala and GABA, whereas *rin* and *Nr* showed the opposite behavior at the same temporal stages. Additionally, *rin* and *Nr* showed lower levels of Thr compared with the wild type, while it was unaltered in *nor*.

During normal Ailsa Craig fruit maturation, the tricarboxylic acid (TCA) cycle intermediates, citrate, isocitrate, succinate, and malate, were highly variable but generally displayed the same behavior as observed in Moneymaker (Carrari et al., 2006). During ripening, we observed a strong increase in the level of succinate. In contrast, malate and isocitrate strongly decreased. All three mutants displayed no alteration in their levels of malate and succinate across the studied period. Furthermore, levels of citrate and isocitrate changed significantly only in *nor*, which displayed the same behavior, albeit to a less dramatic extent compared with the wild type (Fig. 2).

Cell wall-related metabolites, namely Man, Gal, Rha, Rib, Ara, Xyl, and GalUA, increased during normal tomato ripening. This trend is consistent with earlier work, which indicated the particular importance of the degradation of pectin-derived arabinan and galactans during fruit ripening (Sakurai and Nevins, 1993). The levels of these sugars, however, were unaltered in all stages in the mutants, which is again consistent with the characteristic postharvest physiology of these mutants, as they all show substantially reduced pectin degradation (Hobson et al., 1983).

Coordinated Changes of Related Metabolites

In addition to the metabolite changes, we performed a combinatorial analysis of metabolites by subjecting all data points to pairwise correlation analysis. The *nor*, *rin*, and *Nr* mutants showed a total of 520, 864, and 360 significant correlations ($P < 0.05$), respectively. Off these, 450, 686, and 360 were positive ($r^2 > 0.70$) and 70, 178, and 36 were negative ($r^2 < -0.70$), respectively. The full data set of correlation coefficients is presented in the heat maps shown in Figure 3. To simplify the interpretation, metabolites are grouped by compound class. For the *Nr* mutant, the metabolite correlations were performed only in ripening stages (42, 47, 52, and 57 DAP), while for *nor* and *rin*, the analyses were extended to 39, 41, 42, 43, 47, 52, and 57 DAP. In both wild-type sets, all metabolites measured showed significant correlations to compounds outside of their compound class, as was observed previously in cv Moneymaker (Carrari et al., 2006). The individual metabolites with the highest number of correlations were Gly and GABA, with 21 associations in *nor*; Ala, Rib, and Xyl, with 28 associations in *rin*; β-Ala, with 18 associations, and Rha, Ara, and Val, with 17 associations in *Nr*. In general, *Nr* and *nor* displayed far fewer correlations than *rin* or the wild type. *Nr* and *nor* had a considerable number of positive correlations between the levels of various amino acids at different stages of development as well as between amino acids and sugar phosphates, sugar alcohols, and fatty acids, similar to those correlations previously described across development for the wild type (Carrari et al., 2006; Do et al., 2010). That said, the correlations observed for the *rin* data set were much more similar to those seen in the wild type (Carrari et al., 2006; Do et al., 2010), where cell wall-related metabolites, organic acids, and amino acids were highly correlated. As stated above, the "core" metabolite correlations seen in all four genotypes are reminiscent of the metabolites defined to be reflective of development in our previous study of wild-type tomato development (Carrari et al., 2006). Furthermore, the tight correlation of the amino acids is in keeping with both surveys of tomato pericarp metabolite levels in populations of introgression lines resulting from wide crosses of tomato (Carrari et al., 2006; Schauer et al., 2006; Do et al., 2010) and of diverse Arabidopsis genotypes (Sweetlove et al., 2008; Sulpice et al., 2010).

Proteomic Analysis

Pericarp tomato proteins from the wild type and three ripening stages (39, 42, and 52 DAP) in *nor*, *rin*, and *Nr* mutants were treated and labeled using iTRAQ reagents and separated by strong cation-exchange fractionation prior to protein identification and quantifica-

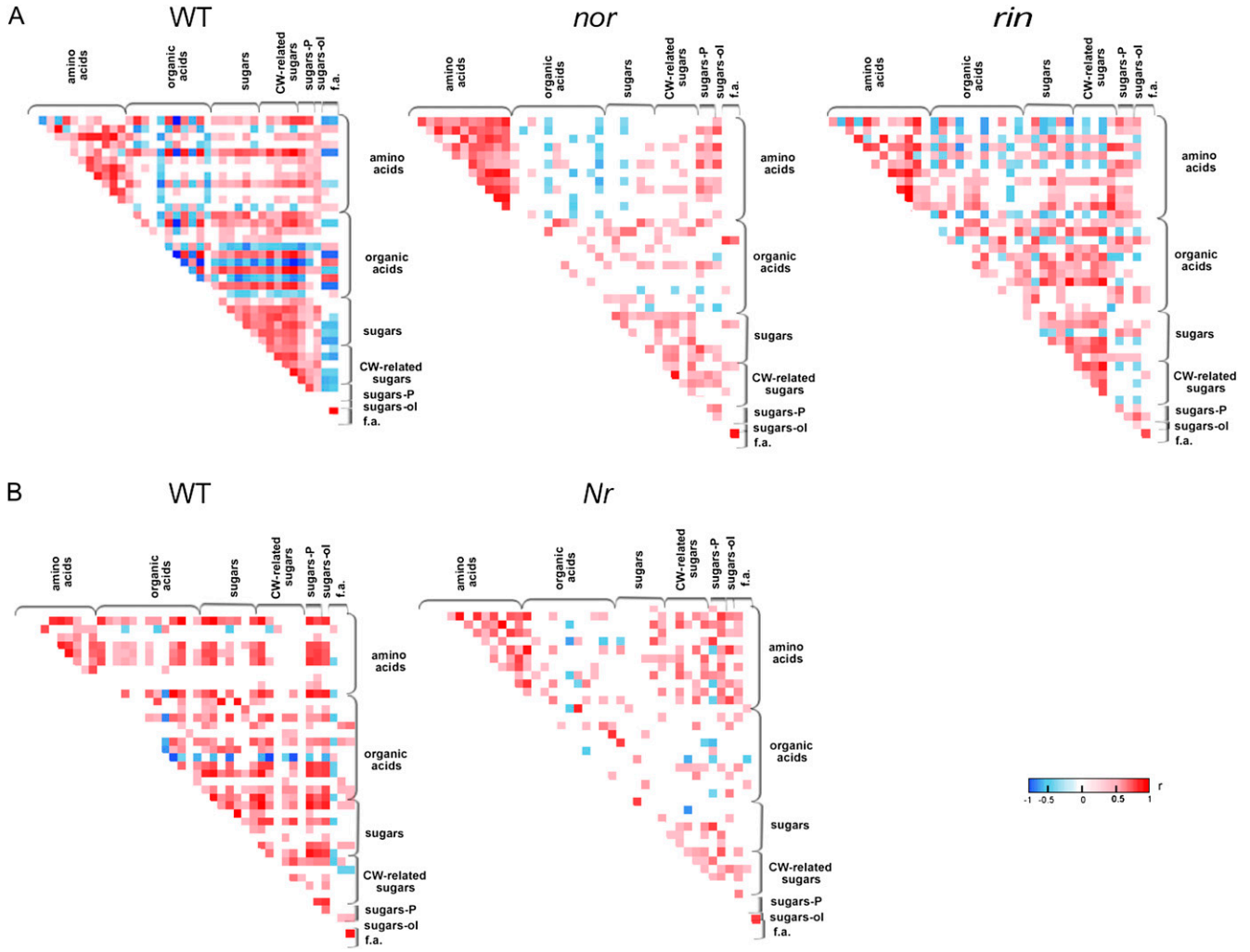

Figure 3. Visualization of metabolite-metabolite correlations. Heat maps of metabolite-metabolite correlations across tomato developmental and ripening stages are shown. For *nor* and *rin*, samples were harvested at 39, 41, 42, 43, 47, 52, and 57 DAP (A), and for *Nr*, samples were harvested at 42, 47, 52, and 57 DAP (B). Metabolites were grouped by compound class, and each square represents the correlation between the metabolite heading the column and the metabolite heading the row. Correlation coefficients and significances were calculated by applying the Pearson algorithm using R. Here, only significant correlations are presented ($P < 0.05$). Positive and negative correlations are presented in red and blue, respectively. WT, Wild type.

tion. This approach, in combination with nano-liquid chromatography (nLC)/electrospray ionization-tandem mass spectrometry (MS/MS), resulted in the identification of 158 differentially expressed proteins (Fig. 4; Supplemental Table S2). As anticipated, *nor* and *rin* are phenotypically similar in terms of fruit and fail to produce climacteric ethylene and responsiveness to ethylene at the molecular level (Lincoln and Fischer, 1988). Combined with the inability to induce ripening in either mutant via exogenous ethylene a regulatory network is defined in which ethylene regulates a subset of ripening genes either directly or in concert with developmental signals influenced by the *nor* and *rin* gene products (Giovannoni, 2004). Based on this regulatory relationships between the *nor* and *rin* genes, a greater number of proteins displayed a similar pattern when comparing *nor* with *rin* than when comparing *nor* with *Nr* or *rin* with *Nr* (Supplemental Fig. S3). In general, we observed that across the three stages analyzed, fruits at the 52-DAP stage showed the highest number of differentially abundant proteins in the mutants compared with the wild type. This total can be subdivided into the 123, 71, and 29 proteins that vary in abundance in *nor*, *rin*, and *Nr* mutants compared with the wild type, respectively. This stage also showed the highest number of common proteins (17) that were detectable in all three genotypes (Supplemental Fig. S3). Of these common proteins, some were related to stress (pathogenesis-related protein, heat shock proteins, glutathione *S*-transferase (GST)-like protein, catalase protein), cell wall metabolism (polygalacturonase), hormone biosynthesis (1-aminocyclopropane-1-carboxylate [ACC] oxidase), and secondary metabolism (flavonoid glucosyltransferase).

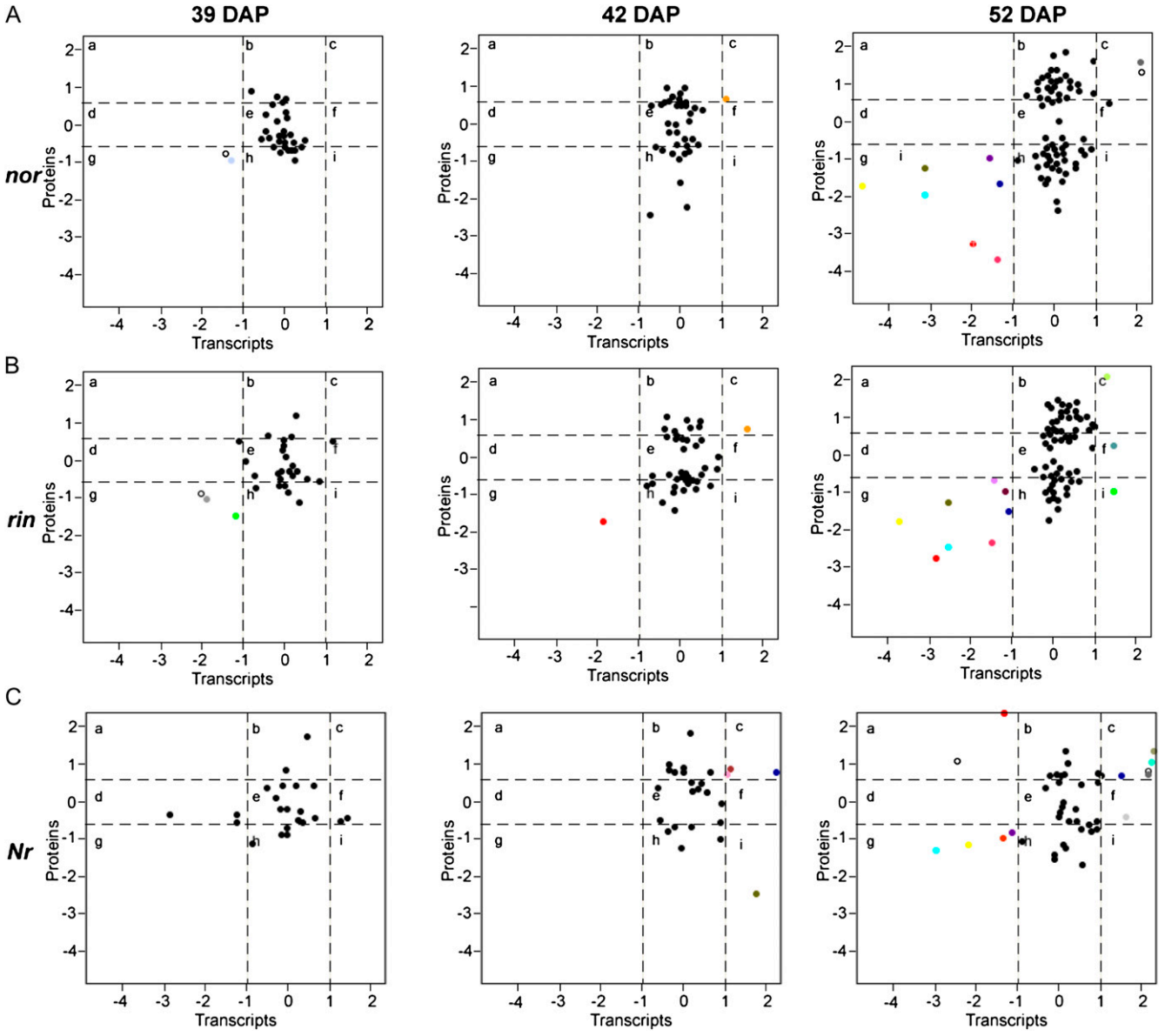

Figure 4. Comparison of changes in mRNA and cognate protein abundance. The relative change in abundance (mutant/wild type) is shown in $\log_2$ scale from samples from 39-, 42-, and 52-DAP tomato fruits: *nor* (A), *rin* (B), and *Nr* (C) mutants. Each color denotes an mRNA-to-protein ratio that was determined to be significant by Student's *t* test analysis ($P < 0.05$) compared with wild-type samples harvested at the same stage: white, Sn-1 (CAA55812); gray, Sn-2 (CAA55813); fluorescent green, heat shock protein (AAD30452); red, polygalacturonase 2 (P05117); blue, pectin esterase (P14280); deep red, Cys proteinase (Q40143); pink, gibberellin 20 oxidase (XP_00251754); dark green, ACC oxidase (ABP68407); dark gray, pathogenesis-related protein P2 (P32045); green-blue, lipoxygenase A (P38415); light gray, lipoxygenase (AAB65766); orange, oxygen-evolving enhancer protein 2 (P29795); yellow, alcohol dehydrogenase (P28032); dark blue, pyruvate decarboxylase (BAC23043); dark lilac, heat shock protein 83 (P51819); dark pink, Met sulfoxide reductase (P54153); dark blue, GST-like protein (AAL92873); brown, pyruvate decarboxylase (AAZ05069); gray-blue, phospho*enol*pyruvate carboxylase 2 (CAB65171); light yellow, ASR4 (AAY98032).

Given that the previously discussed transcript data were obtained from the exact same powdered pericarp samples, we next determined the number of differentially identified proteins for which corresponding transcript probes were represented on the TOM1 array. Of the 158 identified proteins, 133 had representative transcript probes on the microarray. Scatterplot analysis of the $\log_2$-transformed ratios showed the distribution of the corresponding mRNA-to-protein ratios (Fig. 4). At 39 and 42 DAP for all three mutants, almost all mRNA-to-protein ratios were concentrated at the center of the plot (quadrant e), wherein protein and mRNA levels did not vary above 1.5- and 2-fold, respectively. Off center, a total of 45 mRNA-to-protein

ratios across all four genotypes were found in which both the mRNA and protein levels exceeded this level of variation (Table I; Fig. 4). At the 39-DAP stage, it was apparent that all three mutants had fewer mRNA-to-protein ratios outside the central quadrant. In *Nr*, several ratios fell in quadrants b and h, indicating that protein levels were likely up- or down-regulated, but mRNA levels were unchanged. In contrast, *nor* and *rin* were characterized by significant down-regulation of Sn-1 and Sn-2 proteins in both protein and mRNA levels (accession nos. CAA55812 [Sn-1] and CAA55813 [Sn-2]). At 42 DAP, we observed that mRNA-to-protein ratios also mainly fell in quadrants b, e, and h. It follows, therefore, that only a few mRNA-to-protein ratios reflected significant changes at both transcript and protein levels. *Nr* displayed up-regulation at both levels for four proteins: polygalacturonase2 (accession no. P05117), pectinesterase (P14280), Cys proteinase 2 (Q40143), and gibberellin 20 oxidase (XP_00251754). However, contrasting levels were also observed for one gene: up-regulated expression of ACC oxidase (accession no. ABP68407) yet down-regulation of its protein abundance. *nor* and *rin* additionally shared the commonly up-regulated protein, SGRP-1 (accession no. CAA73034), whose transcript was also significantly up-regulated.

The 52-DAP stage was characterized by a large number of mRNA-to-protein ratios falling in the quadrants a, c, g, and i, wherein mRNA-to-protein ratios are substantially different. Moreover, seven down-regulated proteins, which reflected significant down-regulation at the transcript level, were detected in common between *nor* and *rin*, namely pyruvate decarboxylase (BAC23043), GST-like (AAL92873), Met sulfoxide reductase (P54153), polygalacturonase 2 (P05117), heat shock protein 83 (P51819), pyruvate decarboxylase (BAC23043), and alcohol dehydrogenase 2 (P28032). The last three on this list were similarly down-regulated in *Nr*. In addition to these common abundant proteins, aquaporin-like protein (AALD30452) was also down-regulated in *rin* and oxygen-evolving enhancer protein 2 (P29795) was down-regulated in the *Nr* mutant. Additionally, *nor* displayed up-regulation in both protein and transcript levels for Sn-1 (CAA55812) and Sn-2 (CAA55813), as did *Nr*. Moreover, *rin* showed up-regulation of two additional proteins, phospho*enol*pyruvate carboxylase 2 (CAB65171) and ASR4 (AAY98032). Other up-regulated proteins that corresponded to up-regulated transcript expression were also detected in *Nr*, such as pectinesterase 1 (P14280), pathogenesis-related protein P2 (P32045), lipoxygenase A (P38415), and lipoxygenase (AAB65766). Additionally, polygalacturonase 2 (P05117) protein and a small heat shock protein (AAD30452) were down-regulated but showed significant up-regulation at the transcript level in *Nr* and *rin*, respectively. Also, the up-regulated Sh-RNase (BAE92268) protein in *Nr* was down-regulated at the transcriptional level. In summary, these results suggest a substantive degree of posttranscriptional regulatory activity during fruit maturation that has not been described previously in reports focused solely on transcript or protein analysis.

Network Analysis of Transcript, Metabolite, and Protein Levels during Ripening of *nor* and *rin* Tomato Fruits

As is typical of climacteric fruit, ripening in tomato is regulated to a substantial degree by the hormone ethylene. To better understand the ethylene regulatory network, we performed an association study of individual metabolites, a subset of transcript data, and proteins in both the *nor* and *rin* mutants (Supplemental Data Set S2). For the integration analysis, we selected three different stages that covered the ripening process in the wild type: 39 DAP (mature green), 42 DAP (breaker), and 52 DAP (ripe). The data sets used for the correlation comprised 48 metabolites from primary metabolism and a subset of transcripts showing significantly differential expression (178 transcripts for *nor* and 191 for *rin*). The latter included those associated with cell wall metabolism, starch synthesis and degradation, redox stress, polyamine metabolism, transcription factors, fermentation metabolism, TCA cycle, hormone metabolism and signaling, and secondary metabolism. All proteins showing significant differential abundance in the developmental stage studies were selected (154 proteins for *nor* and 121 for *rin*). We analyzed coresponses between metabolic pathway genes, proteins, and metabolites in each genotype (*nor* and *rin*) using a Pearson's correlation coefficient approach at a strict stringency threshold ($P < 0.01$). In each correlation matrix (Fig. 5; Supplemental Fig. S4), transcripts, proteins, and metabolites are represented as nodes (different node shapes represent the different data sets: significant correlations are represented as links that connect the nodes). Network analysis emphasized links both between and within the various types of data. We built the network from each mutant with data relative to wild-type values (transcripts, proteins, and metabolites) in exactly the same way. Interestingly, *nor* revealed markedly higher connectivity than *rin* (*nor* showed a total of 889 links between 357 nodes; *rin* showed a total of 792 links between 354 nodes), suggesting again that NOR may represent a higher level in the regulatory hierarchy as compared with RIN.

Based on our previous results, where a high number of common proteins were found between *nor* and *rin* in the ripe stage (52 DAP), we expected to have a highly significant overlap between the *nor* and *rin* networks. Surprisingly, taking into account the comparative network analysis of three ripening stages when comparing both networks (39, 42, and 52 DAP), we observed different regulation between transcripts, proteins, and metabolites within the three ripening stages (Fig. 5). Comparative network analysis also suggested that in *nor*, associations between nodes were largely modular, while in *rin*, we observed more robust associations between specific metabolites, namely malate, fumarate, Glu, Pro, and Gly (Fig. 5B). The *nor* network analysis revealed two interesting clusters, one of which includes the *Nr* transcript (3.3.1.9; TOM1 identifier SGN-U590044; cluster 1 in Fig. 5A) and another of which

Table I. *Correlation between the expression ratios (mutant/wild type)*

The relative change in abundance (mutant/wild type) is shown in $\log_2$ scale from proteins from 39-, 42-, and 52-DAP tomato fruits. Boldface values denote differences that were determined to be significant by Student's *t* test analysis ($P < 0.05$) compared with wild-type samples harvested at the same stage.

Transcripts ($\log_2$ Fold Change, Mutant Versus Wild Type)	Proteins ($\log_2$ Fold Change, Mutant Versus Wild Type)	GenBank BLAST Annotation		
		Accession no.	Annotation	E value
39 DAP				
nor				
−1.412	**−0.648**	CAA55812	Sn-1	5.00E-20
−1.412	**−0.668**	CAA55813	Sn-2	1.00E-14
rin				
−1.885	**−0.916**	CAA55812	Sn-1	5.00E-20
−1.203	−1.447	AAD30452	Class I small heat shock protein	2.00E-63
−1.885	**−0.874**	CAA55813	Sn-2	1.00E-14
42 DAP				
nor				
1.047	**0.61**	CAA73034	SGRP-1	3.00E-40
rin				
1.607	0.692	CAA73034	SGRP-1	3.00E-40
−1.868	−1.719	P05117	Polygalacturonase 2	4.00E-223
Nr				
1.182	1.219	P05117	Polygalacturonase 2	4.00E-223
2.545	**0.644**	P14280	Pectinesterase 1	0
1.151	0.77	Q40143	Cys proteinase 3	1.00E-196
1.008	0.621	XP_002517541	Gibberellin 20 oxidase	2.00E-64
1.735	−2.489	ABP68407	ACC	3.00E-165
52 DAP				
nor				
2.104	**1.321**	CAA55812	Sn-1	5.00E-20
2.104	**1.636**	CAA55813	Sn-2	1.00E-14
−1.954	**−3.227**	P05117	Polygalacturonase 2	4.00E-223
−4.618	**−1.715**	P28032	Alcohol dehydrogenase 2	5.00E-205
−3.133	**−1.93**	BAC23043	Pyruvate decarboxylase	0
−1.573	**−0.974**	P51819	Heat shock protein	0
−1.407	−3.663	P54153	Peptide Met sulfoxide reductase	3.00E-112
−1.306	**−1.616**	AAL92873	GST-like protein	4.00E-126
−3.133	**−1.249**	AAZ05069	Pyruvate decarboxylase	1.00E-211
rin				
1.04	**0.679**	CAB65171	Phospho*enol*pyruvate carboxylase	0
1.308	**2.04**	AAY98032	ASR4	3.00E-89
−2.832	**−2.797**	P05117	Polygalacturonase 2	4.00E-223
−3.721	**−1.821**	P28032	Alcohol dehydrogenase 2	5.00E-205
−2.532	**−2.442**	BAC23043	Pyruvate decarboxylase	0
−1.132	**−1.019**	P51819	Heat shock protein	0
−1.477	−2.338	P54153	Met sulfoxide reductase	3.00E-112
−1.069	**−1.507**	AAL92873	GST-like protein	4.00E-126
−2.532	**−1.305**	AAZ05069	Pyruvate decarboxylase	1.00E-211
−1.398	−0.686	AAL49750	Aquaporin-like protein	1.00E-145
1.448	−0.998	AAD30452	Small heat shock protein	2.00E-63
Nr				
2.157	**0.863**	CAA55812	Sn-1	5.00E-20
2.917	**0.86**	P14280	Pectinesterase 1	0
2.157	**0.831**	CAA55813	Sn-2	1.00E-14
2.558	**1.416**	P32045	Pathogenesis-related protein P2	4.00E-82
2.16	**1.042**	P38415	Lipoxygenase A	0
1.5	**0.686**	AAB65766	Lipoxygenase	0
−1.359	**−0.995**	P29795	Oxygen-evolving enhancer protein 2, chloroplastic	1.00E-126
−2.213	**−1.17**	P28032	Alcohol dehydrogenase 2	5.00E-205
−2.982	**−1.327**	BAC23043	Pyruvate decarboxylase	0
−1.134	**−0.821**	P51819	Heat shock protein	0
5.572	**−0.967**	P05117	Polygalacturonase 2	4.00E-223
−2.504	1.101	BAE92268	Sh-RNase	6.00E-06

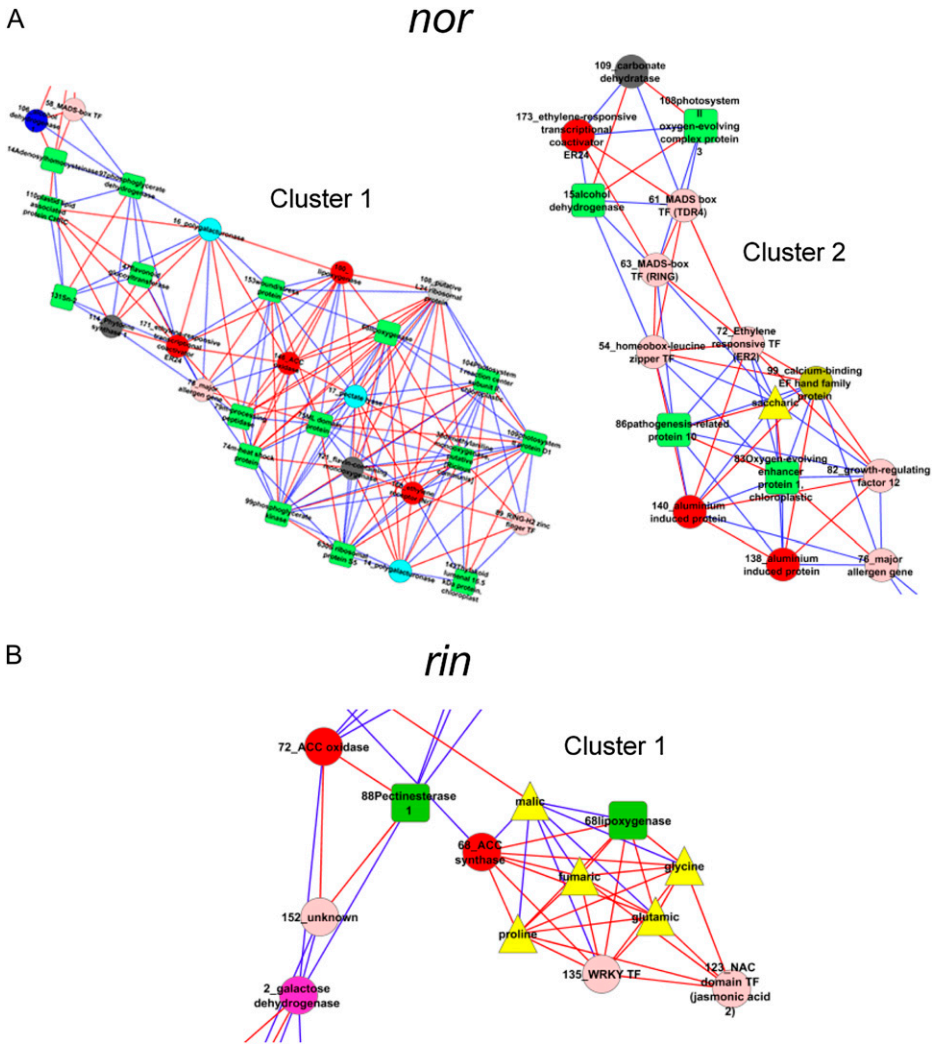

Figure 5. Visualization of transcript-protein-metabolite correlation. Selected clusters are shown from network analysis for *nor* (A) and *rin* (B) at the ripening stages 39, 42, and 52 DAP between select transcript data, all significantly detected proteins, and all measured metabolites (Supplemental Data Set S2). Nodes are as follows: transcripts are represented as circles (light blue, cell wall degradation-related genes; dark pink, cell wall modification-related genes; dark green, major carbohydrate [CHO] metabolism; dark brown, redox stress; light green, polyamine metabolism; light pink, RNA regulation of transcription; light brown, signaling; dark blue, fermentation; light gray, TCA cycle; dark gray, secondary metabolism; red, hormone metabolism), proteins are represented as green squares, and metabolites are represented as yellow triangles. The lines connecting two nodes represent significant correlations: red represents positive and the Pearson algorithm incorporated in R. Here, only significant correlations are presented ($P < 0.01$).

includes *RIN* (8.2.16.2; TOM1 ID SGN-U578471; cluster 2 in Fig. 5A). Interestingly, in the *nor* network (cluster 1), the *Nr* transcript showed coexpression with hormones and cell wall metabolism regulators. The *Nr* transcript level (3.3.1.9; TOM1 ID SGN-U590044) displayed positive correlations with lipoxygenase protein abundance, which is, in turn, positively correlated to lipoxygenase transcript levels (6.4.16.5; TOM1 ID SGN-U578028). The *Nr* transcript also showed positive correlations to the pectin degradation-related genes pectate lyase (1.1.6.7; TOM1 ID SGN-U585252) and polygalacturonase (1.4.12.4; TOM1 ID SGN-U577423). In turn, these pectin degradation-related gene transcripts (pectate lyase, 1.1.6.7; TOM1 ID SGN-U585252; polygalacturonase, 7.4.12.12; TOM1 ID SGN-U577423) showed positive correlation with the hormone-related genes lipoxygenase (6.4.16.5; TOM1 ID SGN-U578028) and ACC oxidase (3.3.4.14; TOM1 ID SGN-U578607). This small regulated cluster was clearly related to primary metabolism, with all these nodes showing a negative correlation with a phosphoglycerate kinase protein. Moreover, the phosphoglycerate kinase protein displayed a positive correlation with PSI reaction subunit II and PSII proteins that are negatively correlated with the *Nr* transcript as well as with cell wall-related genes and lipoxygenase protein.

The other interesting cluster in *nor* contains the *rin* transcription factor (8.2.16.2; TOM1 ID SGN-U578471; cluster 2 in Fig. 5A). Interestingly, the *rin* transcription factor showed a positive correlation with another transcription factor (8.4.16.5; TOM1 ID SGN-U577950), ripening-related transcription factor, fruitfull-like MADS box (Carrari et al., 2006; 3.4.19.21; TOM1 ID SGN-U572851), homobox-Leu zipper protein HAT 22 (4.4.10.20; TOM1 ID SGN-U584756), and ethylene response factor (*ERF2*). Another interesting positive correlation was with an ethylene-responsive transcriptional coactivator, *ER24* (6.1.16.18; TOM1 ID SGN-U566716) as well as other negative correlations with an alcohol dehydrogenase protein related to tomato ripening (Carrari et al., 2006), pathogenesis-related protein 10, and the metabolite saccharinate.

DISCUSSION

Tomato has become the primary experimental model to study fleshy fruit ripening. While earlier studies focused on elucidating ethylene synthesis and signal transduction (Hamilton et al., 1991; Oeller et al., 1991; Picton et al., 1993; Lanahan et al., 1994; Wilkinson et al., 1995; Yen et al., 1995; Lashbrook et al., 1998; Barry et al., 2000; Tieman et al., 2001; Leclercq et al., 2002; Adams-Phillips et al., 2004a; Alba et al., 2005; Zhong et al., 2008) and cell wall-modifying proteins, more recent targets include understanding ripening control upstream of ethylene action, ripening-related signal transduction systems, and downstream metabolic networks. A wide range of studies have shed light on diverse aspects of ripening. The most obvious changes are the transition from partially photosynthetic to fully heterotrophic metabolism (Camara et al., 1995), marked shifts in cell wall composition (Rose et al., 2004a), and other metabolic changes (Giuliano et al., 1993; Fraser et al., 1994; Carrari and Fernie, 2006), all being under strict hormonal regulation of climacteric ripening (Lanahan et al., 1994; Wilkinson et al., 1995; Adams-Phillips et al., 2004a, 2004b; Alba et al., 2004; Barry and Giovannoni, 2006; Giovannoni, 2007; Chung et al., 2010). Together, these data have elucidated how the developmental and ethylene signals are transduced to mediate ripening (for review, see Giovannoni, 2004, 2007; Matas et al., 2009).

Ripening Mutations Provide Tools to Parse Transcription and Hormonal Control

The availability of well-characterized genetic mutants in fruit development and ripening has promoted considerable research on tomato (Giovannoni, 2007). These include two ripening-associated transcription factors, *rin*, which encodes a SEPALLATA MADS box gene (Robinson and Tomes, 1968; Vrebalov et al., 2002), and *nor* (GenBank accession no. AY573802; Tigchelaar et al., 1973), and a two-component His kinase ethylene receptor, *ETR3* (*Nr*; Wilkinson et al., 1995; Yen et al., 1995).

The RIN transcription factor is necessary to induce ripening-associated increases in respiration and ethylene concentration, resulting in fruits that fail to complete normal ripening (Vrebalov et al., 2002; Giovannoni, 2007). Furthermore, fruits remain responsive to ethylene in that ethylene-responsive genes are induced by exogenous ethylene. The ripening regulator transcription factor NOR encodes a NAC domain protein (Tigchelaar et al., 1973, J. Vrebalov and J. Giovannoni, unpublished data). *nor* is phenotypically similar to *rin* in that *nor* fruit fail to produce climacteric ethylene yet show responsiveness to ethylene at the molecular level via ethylene-induced gene expression while remaining unripe in response to ethylene (Lincoln and Fischer, 1988). While *nor* and *rin* may well act together in a cascade to control ripening (Giovannoni, 2007), a number of molecular differences were observed when the expression of ripening-related genes in the presence and absence of exogenous ethylene was examined. Specifically, in mature *nor* fruit, transcripts corresponding to both phytoene synthase (*PSY1*) and the *E8* gene, which are known to be up-regulated during normal ripening (Lincoln et al., 1987), are absent and expression of these genes is not restored by exposing the fruit to ethylene (Yen et al., 1995; Thompson et al., 1999). Similar behavior was observed for the polygalacturonase transcript in the presence and absence of ethylene (Yen et al., 1995; Thompson et al., 1999). However, in *rin*, the effect was not as strong as in *nor*, with *rin* displaying normal induction but reduced levels of expression of *PSY1* and *E8* in mature fruits (Knapp et al., 1989), which could be restored with exogenous ethylene application (Dellapenna et al., 1989). These data suggest that *nor* may have a more global effect on ethylene/ripening-related gene expression than *rin*, in that reduced expression in *rin* reflected the lack of ethylene in these fruit but the lack of expression in *nor*, and the inability to restore expression with ethylene suggests a higher level of control. In the model proposed by Thompson et al. (1999), both genes operate upstream of crucial ripening activity and *nor* is upstream of *rin*, since ethylene/ripening-related gene expression appears to be more extensively inhibited in *nor*.

Ethylene is perceived by two-component His kinase ethylene receptors (Chang and Shockey, 1999), and a mutation in the receptor *LeETR3* (*Nr*) interferes with ethylene perception and, therefore, significantly delays fruit ripening (Lanahan et al., 1994; Wilkinson et al., 1995) and represents a tool to define the fruit ethylene-regulated transcriptome/proteome/metabolome/phenome. Previous transcriptomic, phenotypic, and targeted metabolic analysis revealed that *Nr* influences fruit morphology, seed number, ascorbate accumulation, carotenoid biosynthesis, and ethylene evolution (Alba et al., 2005). Here, we exploited the *rin*, *nor*, and *Nr* mutations to define systems under the influence of transcriptional (*rin* and *nor*) and ethylene (*Nr*) control.

Systems Analysis of Ripening Control Using Ripening Mutations

Here, we utilized an extensive array of tools to characterize the various molecular entities (transcriptome, proteome, metabolome) of the cell (Alba et al., 2004; Fernie et al., 2004; Rose et al., 2004b) in the three ripening tomato mutants, *rin*, *nor*, and *Nr*, with the aim of better understanding transcriptional and ethylene-dependent ripening control. Transcriptional analysis on the three ripening mutants at 10 different developmental stages spanning fruit and ripening revealed how ethylene, via NOR, RIN, and Nr, influences the expression of hundreds of genes during development both prior to the onset of and during ripening. These results corroborate the central role that ethylene plays in governing biochemical, physiological, and developmental processes throughout tomato development.

Different Regulation of Ethylene-Related Genes in *nor*, *rin*, and *Nr*

PageMan analysis of microarray data revealed significant changes in different functional gene categories across the three mutants, supporting overlapping and independent regulatory effects. Regarding ethylene metabolism, and in agreement with previous studies (Wilkinson et al., 1995; Vrebalov et al., 2002), we observed that ethylene-related genes were differentially expressed in the three mutants and as compared with the wild type. During normal development, ethylene synthesis-related genes were up-regulated in breaker stage (42 and 43 DAP) fruits and ethylene signal transduction genes in late ripe stages (47 and 57 DAP). In *Nr*, ethylene synthesis-related genes were strongly up-regulated in a time frame consistent with the normal ripening process (42 DAP) as described by Alba et al. (2005). Interestingly, those genes showed similar up-regulation in *rin* but were unaltered in *nor*, suggesting a response to *nor*-specific activities. Downstream in the ethylene signaling cascade, ethylene signal transduction was apparently unaltered across development and ripening in the three mutants. These data thus support the model postulated by Thompson et al. (1999) where *nor* is a higher order regulator that *rin* or *Nr* (ethylene). Recent chromatin precipitation analysis of RIN protein targets indicates that ethylene synthesis (ACC synthase 2 and 4) gene promoters directly interact with RIN (Fujisawa et al., 2011). This would suggest a linear order of NOR-RIN-NR activity.

Characterization of the Fruit Ethyleneome Demonstrates Regulated Metabolomic Flux toward Ethylene Synthesis

Climacteric ethylene biosynthesis includes the conversion of Asp to Met, the conversion of Met to ethylene, and the Met recycling pathway (Yang and Hoffman, 1984). Ethylene is synthesized from *S*-adenosylmethionine (SAM) by the sequential action of two ethylene biosynthetic enzymes, namely, ACC synthase and ACC oxidase. SAM also has the potential to participate in polyamine or ethylene biosynthesis or both (Mattoo et al., 2007; Mattoo and Handa, 2008). From the transcriptomic and metabolomic data in this study (Figs. 1 and 2), it is apparent that ethylene biosynthesis may dominate the flux through SAM. During normal tomato ripening at the initiation of ethylene biosynthesis, Asp, the precursor of Met, increased in addition to putrescine, one of the three major plant polyamines (Carrari et al., 2006). Asp and putrescine levels were higher in *rin* and *Nr*; however, the changes in Asp levels in the two mutants were far less dramatic than those observed in the wild type, while the change in putrescine was more substantial. Interestingly, these changes in Asp and putrescine correlated with the up-regulation of ethylene synthesis-related genes in *rin* and *Nr*. In contrast, no significant changes in Asp and putrescine levels were observed when comparing *nor* with the wild type, which was mirrored by the lack of change in the expression of ethylene synthesis-related genes in this genotype. These changes are in agreement with a previous study (Mattoo et al., 2007) in which detailed analysis of polyamine accumulation in transgenic tomato lines deficient in the expression of enzymes of polyamine biosynthesis revealed a shift in SAM flux concomitant with an increase of ethylene and a decrease of Asp levels.

nor, *rin*, and *Nr* Displayed Metabolic Shifts

Levels of malate, the precursor of Asp, decreased during ripening in the wild type, as reported previously (Carrari et al., 2006). Malate levels also decreased in *rin* and *Nr*, but the change observed in these mutants was less than that observed in the wild type. In contrast, malate content was unaltered during fruit development in *nor*. These data suggest that ethylene feedback regulates its own synthesis not only at the transcriptional level but also the metabolic level. Another general trend was a general up-regulation of genes related to Suc degradation in *rin* and *Nr* but not in *nor* as well as a down-regulation of aromatic amino acid synthesis-related genes across the late stages of ripening among the three mutants. These changes were reflected in lower Glc and Fru levels, the major hexoses in tomato fruits, in the three mutants in comparison with the wild type. Levels of Phe, the only aromatic amino acid detected in this study, gradually increased during normal ripening and also in the three mutants, but to a lesser extent. Interestingly, aromatic amino acids can act as alternative respiratory substrates when carbohydrates are not abundant (Ishizaki et al., 2005). As such, this decline may reflect a partial reliance of the mitochondrial electron transport chain during later stages of fruit development, when carbon demand is provided entirely by source leaves of the plants, as opposed to a partially autonomous supply of photoassimilates during early fruit development.

Cell Wall Metabolism Is Affected in *nor*, *rin*, and *Nr*

One of the most evident ripening-related changes in tomato fruit is the progressive and extensive loss of firmness, resulting in part from cell wall disassembly (Brummell, 2006; Vicente et al., 2007). Many reports have described modifications to pectic polysaccharides in primary cell walls and middle lamellae, which include the removal of methyl ester groups by pectin esterases, the solubilization of GalUA-rich polysaccharides, and the loss of Gal from pectic fractions (Pressey, 1983; Redgwell et al., 1997). The disassembly of hemicellulosic and pectin cell wall polysaccharides is known to be severely reduced in *rin* fruit and apparently is diminished in *nor*, since they also have only limited softening (Seymour et al., 1987; Giovannoni et al., 1989; Dellapenna et al., 1990; Maclachlan and Brady, 1994). The cell wall-associated transcript, protein, and metabolite data in this study corroborate and extend these previous results. At the transcript

level, we observed up-regulation of the cell wall degradation-related genes polygalacturonase and pectate lyase during ripening in the wild type but not in equivalent-stage *nor* and *rin* fruits, and the up-regulation of these genes was delayed in *Nr*, consistent with the partial ripening response of the mutant. However, at the cell wall-related metabolite level, all three mutants displayed similar patterns during ripening: galacturonate, Gal, Ara, Xyl, Rib, and Rha levels increased substantially during ripening in the wild type, but no such changes were observed in *nor*, *rin*, and *Nr*. These transcript and metabolite data, therefore, indicate that normal ripening-related cell wall degradation is compromised in all three mutants and further suggest that this is an ethylene-influenced phenomenon. Moreover, at the protein level, it has already been shown that in cell wall preparations from normal tomato fruit during ripening, salt-soluble proteins (cell wall-related proteins) were increased (Hobson et al., 1983). However, polygalacturonase-solubilized protein from *rin* was less, and that from the *Nr* cell walls was more, than that from normal wall preparations (Hobson et al., 1983). Similar results were observed in our data: in *Nr*, polygalacturonase and pectin esterase (cell wall degradation-related proteins) were more abundant as compared with the wild type at the breaker stage (42 DAP); however, the opposite behavior was observed at the same stage in *rin*. Moreover, in late ripening stages (52 DAP), a reduction of these proteins was apparent in all three mutants, reflecting that cell wall degradation is likely compromised in these mutants (Dellapenna et al., 1989; Giovannoni et al., 1989). Furthermore, we observed that the reduction in the level of polygalacturonase protein was stronger in *nor* and *rin* as compared with *Nr* at the 52-DAP stage, suggesting that polygalacturonase protein accumulation is influenced by both ethylene and additional transcriptional effects.

Others Metabolic Changes Are Shown by *nor*, *rin*, and *Nr*

In addition to cell wall metabolism per se, the closely related metabolic pathway leading to ascorbate biosynthesis has also been described in ripening tomato fruits (Carrari et al., 2006). We observed an up-regulation of ascorbate-related genes during ripening as well as ascorbate accumulation, as described previously (Alba et al., 2005), only in *Nr*. Interestingly, neither *nor* nor *rin* showed changes in this pathway, suggesting that ascorbate metabolism is influenced by ethylene perception.

PSY1 catalyzes the formation of phytoene, the first C40 carotene intermediate in carotenoid biosynthesis. This is an essential step in the production of the carotenoids, which give the fruit its red color. *Nr*, *nor*, and *rin* all showed some carotenoid production, although the synthesis of lycopene was reduced, delayed, or absent depending on the mutation (Tigchelaar et al., 1973). These phenotypes probably can be explained by the different time frame of expression of *PSY1*. During normal tomato ripening, this gene was induced from breaker stage (42 DAP); however, in *nor* and *rin*, this up-regulation was at earlier stages (39 and 41 DAP, respectively), and in *Nr*, it was at a later stage (52 DAP), again indicating complex ethylene modulation of *PSY1* gene expression.

To date, several studies have indicated that levels of organic acids correlate strongly with genes associated with ethylene and cell wall metabolism-associated pathways, underscoring the importance of these metabolic intermediates in ripening (Carrari et al., 2006; Centeno et al., 2011). In this study, we report than in *nor*, levels of all organic acids, mainly TCA cycle intermediates, were strongly affected across ripening when compared with the wild type, while in *rin* and *Nr*, relatively small changes were observed. These results support the hypothesis that TCA cycle intermediates are regulated at the transcriptional level (Carrari et al., 2006), although we cannot exclude the possibility that in plants, as in animals (He et al., 2004), these intermediates could play a key role in mediating retrograde-regulated gene expression (Zarkovic et al., 2005). Furthermore, the fact that organic acids were more strongly affected in *nor*, a mutant in which ethylene biosynthesis and signaling are also strongly af-

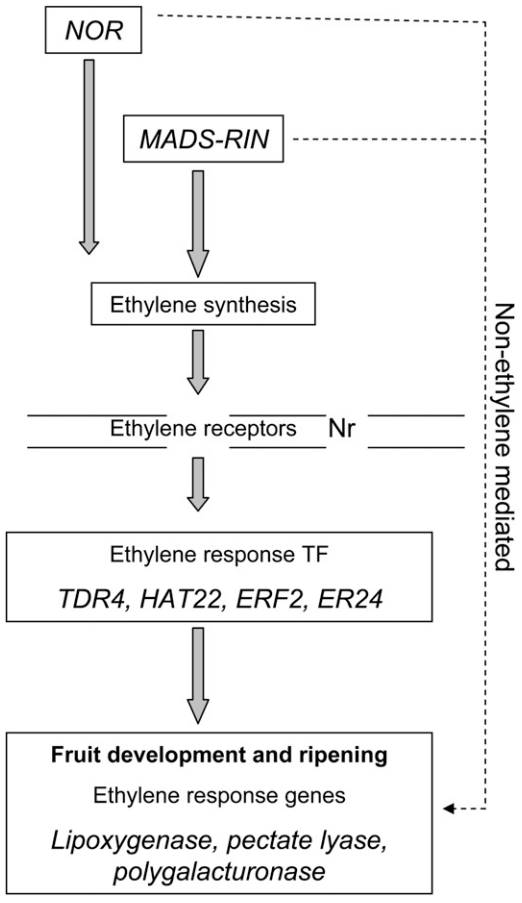

Figure 6. A potential genetic regulatory network centered on ethylene governing tomato fruit development and ripening. TF, Transcription factor.

fected, based on our transcriptomic data, suggests that these metabolites are developmentally regulated at the level of ripening-associated transcripts. This observation has important biotechnological implications, given that the manipulation of organic acids in tomato ripening is relatively facile (Centeno et al., 2011).

Protein Variations as Compared with Transcriptomic Data in *nor*, *rin*, and *Nr*

Transcriptomic profiling allowed the identification of hundreds of genes that were differently regulated during the 10 stages of tomato fruit development among the three mutants. While by no means comprehensive, in this study a total of 158 proteins showed variations in abundance during ripening or equivalent temporal stages of development in *nor*, *rin*, and *Nr* when compared with the wild type. We also found that a similar number of proteins showed decreased or increased expression among the three mutants. The highest number of differently expressed proteins with respect to the wild type were at the ripe stage (52 DAP) among the three mutants. Moreover, *nor* and *rin* shared a greater number of common proteins, especially at 52 DAP (Supplemental Fig. S3). These data further support our conclusion that *nor* and *rin* act together in the ethylene signaling cascade. Of the 158 identified varying proteins, 133 corresponded to gene sequences that figure on the TOM1 microarray, allowing a comparison of ripening-related or genotypic differences in specific transcripts or cognate proteins. In this study, 32% (42 out of 133) of protein and transcript pairs decreased or increased in parallel during ripening. This correlation was particularly apparent at the late ripening stage (52 DAP). A high number of proteins that showed no correlations with the corresponding transcripts belonged to primary metabolism, such as Ser malate dehydrogenase, enolase, glyceraldehyde-3-phosphate dehydrogenase, acid invertase, hydroxymethyltransferase, Glu decarboxylase, and Asp aminotransferase, suggesting that post-transcriptional regulation plays an important role in primary metabolism gene expression and highlighting the need for combined transcriptomic and proteomic analyses.

CONCLUSION

Network analysis revealed key candidate regulators that may play defining roles in tomato fruit ripening. This combination of transcriptome, proteome, and targeted metabolite analysis has helped to refine the ethylene-regulated transcriptome of tomato fruit and added to our knowledge the role of ethylene in both protein and metabolite regulation in tomato ripening. Furthermore, in this study, we were able to draw several important conclusions concerning transcriptomic/metabolic regulation during tomato ripening. First, our data support the contention that *nor* and *rin* act together in a cascade to control ripening (Giovannoni et al., 1995; Thompson et al., 1999) and also suggest that *nor* has a more global effect on ethylene/ripening-related gene expression than *rin*, which indicates that *nor* operates upstream of *rin*. The data also support that *rin* and *nor* act upstream of *Nr*, which would be logically anticipated given the necessity of *rin* and *nor* for ethylene synthesis. A potential genetic regulatory network centered on ethylene governing tomato fruit development and ripening is presented in Figure 6. Third, the metabolite abundance of specific compound classes, such as TCA cycle organic acids and cell wall-related metabolites, appears to be strictly controlled, with specific compounds influenced by ethylene, transcriptional control, or both. Based on an integrated analysis of transcripts, proteins, and metabolites, we were able to identify areas of metabolism that seem to be of high importance to the ripening process, such as hormones and cell wall metabolism in ethylene perception. Therefore, the integrated analysis enables us to uncover additional information for the comprehensive understanding of biological events relevant to metabolic regulation during tomato fruit development. These outputs will provide potential targets for the engineering of metabolism to facilitate the controlled modulation of ripening in tomato fruit.

MATERIALS AND METHODS

Plant Material and Sampling

Tomato (*Solanum lycopersicum* 'Ailsa Craig') and isogenic lines for *nor*, *rin*, and *Nr* mutations (cv Ailsa Craig, backcross parent) were grown in the greenhouse at 26°C under 12 h of supplemental lighting followed by 12 h at 20°C. To collect stages prior to ripening, fruits were tagged at 7 DAP (fruit less than 1 cm; Giovannoni et al., 1989) and harvested at one of the following 10 time points: 7, 17, 27, 39 (mature green), 41 (breaker − 1), 42 (breaker), 43 (breaker + 1), 47 (breaker + 5), 52 (breaker + 10), and 57 (breaker + 15) DAP. The first signs of carotenoid accumulation on the external surface of the fruit were taken to define the breaker stage. To maximize developmental synchrony, harvested fruit were visually inspected externally and internally (e.g. size, shape, pigmentation, seed development, and development of locular jelly), and only fruits appearing developmentally equivalent were kept for the analysis. Transcriptome, proteome, and metabolome analyses were performed in the same material. For the *Nr* mutant, analysis was performed in three separate pools of fruits of 15 to 30 fruit each. All fruits were collected from four individual plants. For *nor* and *rin* mutants, eight to 10 individual fruits for each time point were considered as biological replicates. These individual fruit replicates came from 10 to 15 *rin*, *nor*, and wild-type plants (all of which were grown in the greenhouse crop; the genotypes were randomly distributed in the greenhouse).

For transcriptome, proteome, and metabolome analyses, eight, four, and five biological replicates were used. After tissue selection, pericarp tissue was collected, frozen in liquid nitrogen, and stored at −80°C until further analysis.

Transcriptome Analysis

Total RNA from tomato pericarp was extracted as described by Alba et al. (2004, 2005). cDNA synthesis, labeling, hybridization, washes, and scanning were conducted as described (Alba et al., 2004). Glass slides containing arrayed tomato ESTs were obtained directly from the Center for Gene Expression Profiling at the Boyce Thompson Institute, synthesized in the Giovannoni laboratory as described by Alba et al. (2004). The tomato array (TOM1) contains approximately 12,000 unique elements randomly selected

from cDNA libraries isolated from a range of tissues, including leaf, root, fruit, and flower and representing a broad range of metabolic and developmental processes. Nucleic acid sequence and annotation data pertaining to the TOM1 microarray are available via the Tomato Functional Genomics Database (http://ted.bti.cornell.edu). Data acquisition and filtering were conducted as described (Alba et al., 2005). The raw intensity values were normalized using Robin's default settings for two-color microarray analysis (Lohse et al., 2010). Specifically, background intensities were subtracted from the foreground values, and subsequently, a print tip-wise Loess normalization (Yang et al., 2002) was performed within each array. To reduce technical variation between chips, the logarithmized red and green channel intensity ratios on each chip were subsequently scaled across all arrays (Yang et al., 2002; Smyth and Speed, 2003) to have the same median absolute deviation. Statistical analysis of differential gene expression was carried out using the linear model-based approach developed by Smyth (2004). The obtained *P* values were corrected for multiple testing using the strategy described by Benjamini and Hochberg (1995) separately for each of the comparisons made. Genes that showed an absolute $\log_2$ fold-change value of at least 1 and a *P* value lower than 0.05 were considered significantly differentially expressed. The $\log_2$ fold-change cutoff value was imposed to account for noise in the experiment and to make sure that only genes that show a marked reaction were recorded. For visualization, the data were loaded into MapMan (Usadel et al., 2009), which displays individual genes mapped on their pathways as false-color-coded rectangles. MapMan bins were assigned to each cDNA on the glass based on the SGN tomato unigene mapping. Wilcoxon rank sum tests were performed to test whether there were bins that were significantly and consistently different from the other bins in the MapMan ontology using the built-in function in MapMan. The PageMan software package (Usadel et al., 2006) was then used to select and display biologically relevant details of these data sets. The transcript data for *Nr* has previously been published (Alba et al., 2005). The design of *nor* and *rin* microarrays was performed using RNA pooled from different tissues (a combination of tissues from different developmental stages of pericarp, leaf, and stem tissue) as a reference.

Proteome Analysis

Proteins were extracted from pericarp tissues of mature green, breaker, and breaker + 10 stages from four biological replicates of the wild type and the *nor*, *rin*, and *Nr* mutants. Samples were prepared as described (Isaacson et al., 2006). Extracted proteins were quantified using a modified Bradford method (Bradford, 1976). In order to confirm the quantification, 20 μg of each sample was loaded on a 12% acrylamide gel and run under denaturing conditions. The gel was stained with 0.04% Coomassie blue R-250 staining solution and analyzed using ImageJ software (Abramoff et al., 2004). Protein preparation and identification were done as described by G. López-Casado, P.A. Covey, P.A. Bedinger, L.A. Mueller, Z. Fei, J.J. Giovannoni, and J.K.C. Rose (unpublished data). Proteins were labeled using the iTRAQ (Isobaric Tag for Relative and Absolute Quantitation) Reagents Multiplex kit (Applied Biosystems) according to the manufacturer's instructions and digested with trypsin. Labeled peptide mixtures were first analyzed by matrix-assisted laser-desorption ionization time of flight MS (ABI 4700; Applied Biosystems) to confirm digestion and labeling. A strong cation-exchange fractionation LC apparatus using an Agilent 1100 HPLC device with a UV detector (Agilent Technologies) was followed by nLC-MS/MS. All nLC-MS/MS experiments were performed using an LC Packings Ultimate integrated capillary HPLC system equipped with a Switchos valve switching unit (Dionex) connected in line to a hybrid triple quadrupole linear ion-trap mass spectrometer (4000 Q Trap; ABI/MDS Sciex) and equipped with a Micro Ion Spray Head ion source. MS data acquisition was performed using Analyst 1.4.2 software (Applied Biosystems) in the positive ion mode for information-dependent acquisition analysis. MS data were interrogated using the paragon method (Shilov et al., 2007) using ProteinPilot software 2.0 (Applied Biosystems) and searched against a translated custom unigene database derived from the RNA-sEquation (454 pyrosequencing; GS FLX; Roche) database (Assembly2009_protein; ftp://ted.bti.cornell.edu/pub/tomato_454_unigene/). Only proteins showing a protein score higher than 95% (or 1.3 in ProteinPilot) with two or more unique peptides identified with a *P* value of 0.05 or less, and false discovery rate of less than 0.15, were further analyzed.

Metabolome Analysis

Metabolite analysis by GC-MS was carried out essentially as described (Lisec et al., 2006) but with modifications specific for tomato (Schauer et al., 2006). The mass spectra were cross-referenced with those in the Golm Metabolome Database (Kopka et al., 2005). Analyses of primary metabolites were done in pericarp tissue from 27, 39, 41, 42, 43, 47, 52, and 57 DAP in lines for *nor* and *rin* mutations and from 42, 47, 52, and 57 DAP from the *Nr* mutation. Each sample point was analyzed with five biological replicates.

Data Analysis and Statistics

Data normalization, visualization, heat maps, and correlation analysis based on Pearson correlation were performed using R software (Gentleman, 1996). Visualization of transcript-protein-metabolite correlation was conducted using Cytoscape (Cline et al., 2007).

Supplemental Data

The following materials are available in the online version of this article.

Supplemental Figure S1. A condensed PageMap display of changed pathways.

Supplemental Figure S2. A condensed PageMap display of altered pathways that are not represented in Figure 1.

Supplemental Figure S3. Venn diagrams of proteins that increased or decreased among the three mutants.

Supplemental Figure S4. Visualization of transcript-protein-metabolite correlation.

Supplemental Table S1. Raw data from PageMan analysis (Fig. 1; Supplemental Fig. S2).

Supplemental Table S2. Total significantly detected proteins among the three mutants relative to the wild type.

Supplemental Data Set S1. Transcriptome data set.

Supplemental Data Set S2. Selected transcripts and proteins for network analysis.

Supplemental Data Set S3. Primary metabolite levels in the wild type, *nor*, *rin*, and *Nr* (metabolites not presented in Fig. 2).

Supplemental File S1. MapMan (http://mapman.gabipd.org/web/guest/mapmanweb).

ACKNOWLEDGMENTS

We thank Axel Nagel for online data deposition.

Received March 1, 2011; accepted July 24, 2011; published July 27, 2011.

LITERATURE CITED

Abramoff MD, Magelhaes PJ, Ram SJ (2004) Image processing with ImageJ. Biophotonics Int **11:** 36–42

Adams-Phillips L, Barry C, Giovannoni J (2004a) Signal transduction systems regulating fruit ripening. Trends Plant Sci **9:** 331–338

Adams-Phillips L, Barry C, Kannan P, Leclercq J, Bouzayen M, Giovannoni J (2004b) Evidence that CTR1-mediated ethylene signal transduction in tomato is encoded by a multigene family whose members display distinct regulatory features. Plant Mol Biol **54:** 387–404

Alba R, Fei Z, Payton P, Liu Y, Moore SL, Debbie P, Cohn J, D'Ascenzo M, Gordon JS, Rose JK, et al (2004) ESTs, cDNA microarrays, and gene expression profiling: tools for dissecting plant physiology and development. Plant J **39:** 697–714

Alba R, Payton P, Fei Z, McQuinn R, Debbie P, Martin GB, Tanksley SD, Giovannoni JJ (2005) Transcriptome and selected metabolite analyses reveal multiple points of ethylene control during tomato fruit development. Plant Cell **17:** 2954–2965

Amor Y, Haigler CH, Johnson S, Wainscott M, Delmer DP (1995) A membrane-associated form of sucrose synthase and its potential role in synthesis of cellulose and callose in plants. Proc Natl Acad Sci USA **92:** 9353–9357

Armengaud P, Sulpice R, Miller AJ, Stitt M, Amtmann A, Gibon Y (2009) Multilevel analysis of primary metabolism provides new insights into the role of potassium nutrition for glycolysis and nitrogen assimilation in Arabidopsis roots. Plant Physiol **150:** 772–785

Barry CS, Giovannoni JJ (2006) Ripening in the tomato Green-ripe mutant is inhibited by ectopic expression of a protein that disrupts ethylene signaling. Proc Natl Acad Sci USA **103:** 7923–7928

Barry CS, Llop-Tous MI, Grierson D (2000) The regulation of 1-aminocyclopropane-1-carboxylic acid synthase gene expression during the transition from system-1 to system-2 ethylene synthesis in tomato. Plant Physiol **123:** 979–986

Barry CS, McQuinn RP, Chung MY, Besuden A, Giovannoni JJ (2008) Amino acid substitutions in homologs of the STAY-GREEN protein are responsible for the green-flesh and chlorophyll retainer mutations of tomato and pepper. Plant Physiol **147:** 179–187

Benjamini Y, Hochberg Y (1995) Controlling the false discovery rate: a practical and powerful approach to multiple testing. J R Stat Soc B **57:** 289–300

Bradford MM (1976) A rapid and sensitive method for the quantitation of microgram quantities of protein utilizing the principle of protein-dye binding. Anal Biochem **72:** 248–254

Brummell DA (2006) Cell wall disassembly in ripening fruit. Funct Plant Biol **33:** 103–119

Camara B, Hugueney P, Bouvier F, Kuntz M, Monéger R (1995) Biochemistry and molecular biology of chromoplast development. Int Rev Cytol **163:** 175–247

Carrari F, Baxter C, Usadel B, Urbanczyk-Wochniak E, Zanor MI, Nunes-Nesi A, Nikiforova V, Centero D, Ratzka A, Pauly M, et al (2006) Integrated analysis of metabolite and transcript levels reveals the metabolic shifts that underlie tomato fruit development and highlight regulatory aspects of metabolic network behavior. Plant Physiol **142:** 1380–1396

Carrari F, Fernie AR (2006) Metabolic regulation underlying tomato fruit development. J Exp Bot **57:** 1883–1897

Centeno DC, Osorio S, Nunes-Nesi A, Bertolo AL, Carneiro RT, Araújo WL, Steinhauser MC, Michalska J, Rohrmann J, Geigenberger P, et al (2011) Malate plays a crucial role in starch metabolism, ripening, and soluble solid content of tomato fruit and affects postharvest softening. Plant Cell **23:** 162–184

Chaabouni S, Jones B, Delalande C, Wang H, Li Z, Mila I, Frasse P, Latché A, Pech JC, Bouzayen M (2009) Sl-IAA3, a tomato Aux/IAA at the crossroads of auxin and ethylene signalling involved in differential growth. J Exp Bot **60:** 1349–1362

Chang C, Shockey JA (1999) The ethylene-response pathway: signal perception to gene regulation. Curr Opin Plant Biol **2:** 352–358

Chung MY, Vrebalov J, Alba R, Lee J, McQuinn R, Chung JD, Klein P, Giovannoni J (2010) A tomato (Solanum lycopersicum) APETALA2/ERF gene, SlAP2a, is a negative regulator of fruit ripening. Plant J **64:** 936–947

Cline MS, Smoot M, Cerami E, Kuchinsky A, Landys N, Workman C, Christmas R, Avila-Campilo I, Creech M, Gross B, et al (2007) Integration of biological networks and gene expression data using Cytoscape. Nat Protoc **2:** 2366–2382

Dellapenna D, Lashbrook CC, Toenjes K, Giovannoni JJ, Fischer RL, Bennett AB (1990) Polygalacturonase isozymes and pectin depolymerization in transgenic rin tomato fruit. Plant Physiol **94:** 1882–1886

Dellapenna D, Lincoln JE, Fischer RL, Bennett AB (1989) Transcriptional analysis of polygalacturonase and other ripening associated genes in Rutgers, rin, nor, and Nr tomato fruit. Plant Physiol **90:** 1372–1377

Do PT, Prudent M, Sulpice R, Causse M, Fernie AR (2010) The influence of fruit load on the tomato pericarp metabolome in a Solanum chmielewskii introgression line population. Plant Physiol **154:** 1128–1142

Enfissi EM, Barneche F, Ahmed I, Lichtlé C, Gerrish C, McQuinn RP, Giovannoni JJ, Lopez-Juez E, Bowler C, Bramley PM, et al (2010) Integrative transcript and metabolite analysis of nutritionally enhanced DE-ETIOLATED1 downregulated tomato fruit. Plant Cell **22:** 1190–1215

Fait A, Hanhineva K, Beleggia R, Dai N, Rogachev I, Nikiforova VJ, Fernie AR, Aharoni A (2008) Reconfiguration of the achene and receptacle metabolic networks during strawberry fruit development. Plant Physiol **148:** 730–750

Faurobert M, Mihr C, Bertin N, Pawlowski T, Negroni L, Sommerer N, Causse M (2007) Major proteome variations associated with cherry tomato pericarp development and ripening. Plant Physiol **143:** 1327–1346

Fernandez AI, Viron N, Alhagdow M, Karimi M, Jones M, Amsellem Z, Sicard A, Czerednik A, Angenent G, Grierson D, et al (2009) Flexible tools for gene expression and silencing in tomato. Plant Physiol **151:** 1729–1740

Fernie AR, Trethewey RN, Krotzky AJ, Willmitzer L (2004) Metabolite profiling: from diagnostics to systems biology. Nat Rev Mol Cell Biol **5:** 763–769

Fraser PD, Enfissi EM, Halket JM, Truesdale MR, Yu D, Gerrish C, Bramley PM (2007) Manipulation of phytoene levels in tomato fruit: effects on isoprenoids, plastids, and intermediary metabolism. Plant Cell **19:** 3194–3211

Fraser PD, Truesdale MR, Bird CR, Schuch W, Bramley PM (1994) Carotenoid biosynthesis during tomato fruit development (evidence for tissue-specific gene expression). Plant Physiol **105:** 405–413

Fujisawa M, Nakano T, Ito Y (2011) Identification of potential target genes for the tomato fruit-ripening regulator RIN by chromatin immunoprecipitation. BMC Plant Biol **11:** 26

Gentleman RI (1996) R: a language for data analysis and graphics. J Comput Graph Statist **5:** 299–314

Gillaspy G, Ben-David HM, Gruissem W (1993) Fruits: a developmental perspective. Plant Cell **5:** 1439–1451

Giovannoni JJ (2004) Genetic regulation of fruit development and ripening. Plant Cell (Suppl) **16:** S170–S180

Giovannoni JJ (2007) Fruit ripening mutants yield insights into ripening control. Curr Opin Plant Biol **10:** 283–289

Giovannoni JJ, DellaPenna D, Bennett AB, Fischer RL (1989) Expression of a chimeric polygalacturonase gene in transgenic rin (ripening inhibitor) tomato fruit results in polyuronide degradation but not fruit softening. Plant Cell **1:** 53–63

Giovannoni JJ, Noensie EN, Ruezinsky DM, Lu X, Tracy SL, Ganal MW, Martin GB, Pillen K, Alpert K, Tanksley SD (1995) Molecular genetic analysis of the ripening-inhibitor and non-ripening loci of tomato: a first step in genetic map-based cloning of fruit ripening genes. Mol Gen Genet **248:** 195–206

Giuliano G, Bartley GE, Scolnik PA (1993) Regulation of carotenoid biosynthesis during tomato development. Plant Cell **5:** 379–387

Goff SA, Klee HJ (2006) Plant volatile compounds: sensory cues for health and nutritional value? Science **311:** 815–819

Hamilton AJ, Bouzayen M, Grierson D (1991) Identification of a tomato gene for the ethylene-forming enzyme by expression in yeast. Proc Natl Acad Sci USA **88:** 7434–7437

He W, Miao FJ, Lin DC, Schwandner RT, Wang Z, Gao J, Chen JL, Tian H, Ling L (2004) Citric acid cycle intermediates as ligands for orphan G-protein-coupled receptors. Nature **429:** 188–193

Hobson GE, Richardson C, Gillham DJ (1983) Release of protein from normal and mutant tomato cell walls. Plant Physiol **71:** 635–638

Isaacson T, Damasceno CM, Saravanan RS, He Y, Catalá C, Saladié M, Rose JK (2006) Sample extraction techniques for enhanced proteomic analysis of plant tissues. Nat Protoc **1:** 769–774

Ishizaki K, Larson TR, Schauer N, Fernie AR, Graham IA, Leaver CJ (2005) The critical role of Arabidopsis electron-transfer flavoprotein: ubiquinone oxidoreductase during dark-induced starvation. Plant Cell **17:** 2587–2600

Karlova R, Rosin FM, Busscher-Lange J, Parapunova V, Do PT, Fernie AR, Fraser PD, Baxter C, Angenent GC, de Maagd RA (2011) Transcriptome and metabolite profiling show that APETALA2a is a major regulator of tomato fruit ripening. Plant Cell **23:** 923–941

Knapp J, Moureau P, Schuch W, Grierson D (1989) Organisation and expression of polygalacturonase and other ripening genes in Ailsa Craig 'Neverripe' and 'ripening inhibitor' tomato mutants. Plant Mol Biol **12:** 105–116

Kopka J, Schauer N, Krueger S, Birkemeyer C, Usadel B, Bergmüller E, Dörmann P, Weckwerth W, Gibon Y, Stitt M, et al (2005) GMD@CSB.DB: the Golm Metabolome Database. Bioinformatics **21:** 1635–1638

Lanahan MB, Yen HC, Giovannoni JJ, Klee HJ (1994) The never ripe mutation blocks ethylene perception in tomato. Plant Cell **6:** 521–530

Lashbrook CC, Tieman DM, Klee HJ (1998) Differential regulation of the tomato ETR gene family throughout plant development. Plant J **15:** 243–252

Leclercq J, Adams-Phillips LC, Zegzouti H, Jones B, Latché A, Giovannoni JJ, Pech JC, Bouzayen M (2002) LeCTR1, a tomato CTR1-like gene, demonstrates ethylene signaling ability in Arabidopsis and novel expression patterns in tomato. Plant Physiol **130:** 1132–1142

Lemaire-Chamley M, Petit J, Garcia V, Just D, Baldet P, Germain V, Fagard M, Mouassite M, Cheniclet C, Rothan C (2005) Changes in

transcriptional profiles are associated with early fruit tissue specialization in tomato. Plant Physiol **139:** 750–769

Lincoln JE, Cordes S, Read E, Fischer RL (1987) Regulation of gene expression by ethylene during Lycopersicon esculentum (tomato) fruit development. Proc Natl Acad Sci USA **84:** 2793–2797

Lincoln JE, Fischer RL (1988) Diverse mechanisms for the regulation of ethylene-inducible gene expression. Mol Gen Genet **212:** 71–75

Lisec J, Schauer N, Kopka J, Willmitzer L, Fernie AR (2006) Gas chromatography mass spectrometry-based metabolite profiling in plants. Nat Protoc **1:** 387–396

Liu Y, Roof S, Ye Z, Barry C, van Tuinen A, Vrebalov J, Bowler C, Giovannoni J (2004) Manipulation of light signal transduction as a means of modifying fruit nutritional quality in tomato. Proc Natl Acad Sci USA **101:** 9897–9902

Lohse M, Nunes-Nesi A, Krüger P, Nagel A, Hannemann J, Giorgi FM, Childs L, Osorio S, Walther D, Selbig J, et al (2010) Robin: an intuitive wizard application for R-based expression microarray quality assessment and analysis. Plant Physiol **153:** 642–651

Maclachlan G, Brady C (1994) Endo-1,4-β-glucanase, xyloglucanase, and xyloglucan endo-transglycosylase activities versus potential substrates in ripening tomatoes. Plant Physiol **105:** 965–974

Manning K, Tör M, Poole M, Hong Y, Thompson AJ, King GJ, Giovannoni JJ, Seymour GB (2006) A naturally occurring epigenetic mutation in a gene encoding an SBP-box transcription factor inhibits tomato fruit ripening. Nat Genet **38:** 948–952

Martí C, Orzáez D, Ellul P, Moreno V, Carbonell J, Granell A (2007) Silencing of DELLA induces facultative parthenocarpy in tomato fruits. Plant J **52:** 865–876

Matas AJ, Gapper NE, Chung MY, Giovannoni JJ, Rose JK (2009) Biology and genetic engineering of fruit maturation for enhanced quality and shelf-life. Curr Opin Biotechnol **20:** 197–203

Mattoo AK, Chung SH, Goyal RK, Fatima T, Solomos T, Srivastava A, Handa AK (2007) Overaccumulation of higher polyamines in ripening transgenic tomato fruit revives metabolic memory, upregulates anabolism-related genes, and positively impacts nutritional quality. J AOAC Int **90:** 1456–1464

Mattoo AK, Handa AK (2008) Higher polyamines restore and enhance metabolic memory in ripening fruit. Plant Sci **174:** 386–393

Moco S, Capanoglu E, Tikunov Y, Bino RJ, Boyacioglu D, Hall RD, Vervoort J, De Vos RC (2007) Tissue specialization at the metabolite level is perceived during the development of tomato fruit. J Exp Bot **58:** 4131–4146

Moing A, Aharoni A, Biais B, Rogachev I, Meir S, Brodsky L, Allwood JW, Erban A, Dunn WB, Kay L, et al (2011) Extensive metabolic cross-talk in melon fruit revealed by spatial and developmental combinatorial metabolomics. New Phytol **190:** 683–696

Mustilli AC, Fenzi F, Ciliento R, Alfano F, Bowler C (1999) Phenotype of the tomato high pigment-2 mutant is caused by a mutation in the tomato homolog of DEETIOLATED1. Plant Cell **11:** 145–157

Nashilevitz S, Melamed-Bessudo C, Izkovich Y, Rogachev I, Osorio S, Itkin M, Adato A, Pankratov I, Hirschberg J, Fernie AR, et al (2010) An orange ripening mutant links plastid NAD(P)H dehydrogenase complex activity to central and specialized metabolism during tomato fruit maturation. Plant Cell **22:** 1977–1997

Niittylä T, Messerli G, Trevisan M, Chen J, Smith AM, Zeeman SC (2004) A previously unknown maltose transporter essential for starch degradation in leaves. Science **303:** 87–89

Oeller PW, Lu MW, Taylor LP, Pike DA, Theologis A (1991) Reversible inhibition of tomato fruit senescence by antisense RNA. Science **254:** 437–439

Page D, Gouble B, Valot B, Bouchet JP, Callot C, Kretzschmar A, Causse M, Renard CM, Faurobert M (2010) Protective proteins are differentially expressed in tomato genotypes differing for their tolerance to low-temperature storage. Planta **232:** 483–500

Picton S, Gray J, Barton S, AbuBakar U, Lowe A, Grierson D (1993) cDNA cloning and characterisation of novel ripening-related mRNAs with altered patterns of accumulation in the ripening inhibitor (rin) tomato ripening mutant. Plant Mol Biol **23:** 193–207

Pressey R (1983) β-Galactosidases in ripening tomatoes. Plant Physiol **71:** 132–135

Redgwell RJ, MacRae E, Hallett I, Fischer M, Perry J, Harker R (1997) In vivo and in vitro swelling of cell walls during fruit ripening. Planta **203:** 162–173

Reiter WD (2008) Biochemical genetics of nucleotide sugar interconversion reactions. Curr Opin Plant Biol **11:** 236–243

Robinson R, Tomes M (1968) Ripening inhibitor: a gene with multiple effects on ripening. Rep Tomato Genet Coop **18:** 36–37

Roessner-Tunali U, Hegemann B, Lytovchenko A, Carrari F, Bruedigam C, Granot D, Fernie AR (2003) Metabolic profiling of transgenic tomato plants overexpressing hexokinase reveals that the influence of hexose phosphorylation diminishes during fruit development. Plant Physiol **133:** 84–99

Rose JK, Saladié M, Catalá C (2004a) The plot thickens: new perspectives of primary cell wall modification. Curr Opin Plant Biol **7:** 296–301

Rose JKC, Bashir S, Giovannoni JJ, Jahn MM, Saravanan RS (2004b) Tackling the plant proteome: practical approaches, hurdles and experimental tools. Plant J **39:** 715–733

Rose JKC, Bennett AB (1999) Cooperative disassembly of the cellulose-xyloglucan network of plant cell walls: parallels between cell expansion and fruit ripening. Trends Plant Sci **4:** 176–183

Sakurai N, Nevins DJ (1993) Changes in physical properties and cell wall polysaccharides of tomato (Lycopersicon esculentum) pericarp tissues. Physiol Plant **89:** 681–686

Saravanan RS, Rose JK (2004) A critical evaluation of sample extraction techniques for enhanced proteomic analysis of recalcitrant plant tissues. Proteomics **4:** 2522–2532

Schauer N, Semel Y, Roessner U, Gur A, Balbo I, Carrari F, Pleban T, Perez-Melis A, Bruedigam C, Kopka J, et al (2006) Comprehensive metabolic profiling and phenotyping of interspecific introgression lines for tomato improvement. Nat Biotechnol **24:** 447–454

Seymour G (1993) Biochemistry of Fruit Ripening. Chapman and Hall, London

Seymour GB, Harding SE, Taylor AJ, Hobson GE, Tucker GA (1987) Polyuronide solubilization during ripening of normal and mutant tomato fruit. Phytochemistry **144:** 1871–1875

Shilov IV, Seymour SL, Patel AA, Loboda A, Tang WH, Keating SP, Hunter CL, Nuwaysir LM, Schaeffer DA (2007) The Paragon Algorithm, a next generation search engine that uses sequence temperature values and feature probabilities to identify peptides from tandem mass spectra. Mol Cell Proteomics **6:** 1638–1655

Smyth GK (2004) Linear models and empirical Bayes methods for assessing differential expression in microarray experiments. Stat Appl Genet Mol Biol **3:** Article 3

Smyth GK, Speed T (2003) Normalization of cDNA microarray data. Methods **31:** 265–273

Sulpice R, Trenkamp S, Steinfath M, Usadel B, Gibon Y, Witucka-Wall H, Pyl ET, Tschoep H, Steinhauser MC, Guenther M, et al (2010) Network analysis of enzyme activities and metabolite levels and their relationship to biomass in a large panel of *Arabidopsis* accessions. Plant Cell **22:** 2872–2893

Sweetlove LJ, Fell D, Fernie AR (2008) Getting to grips with the plant metabolic network. Biochem J **409:** 27–41

Thompson AJ, Tor M, Barry CS, Vrebalov J, Orfila C, Jarvis MC, Giovannoni JJ, Grierson D, Seymour GB (1999) Molecular and genetic characterization of a novel pleiotropic tomato-ripening mutant. Plant Physiol **120:** 383–390

Tieman DM, Ciardi JA, Taylor MG, Klee HJ (2001) Members of the tomato LeEIL (EIN3-like) gene family are functionally redundant and regulate ethylene responses throughout plant development. Plant J **26:** 47–58

Tigchelaar EC, Tomes M, Kerr EA, Barman RJ (1973) A new fruit ripening mutant, non-ripening (nor). Rep Tomato Genet Coop **23:** 33–34

Usadel B, Nagel A, Steinhauser D, Gibon Y, Bläsing OE, Redestig H, Sreenivasulu N, Krall L, Hannah MA, Poree F, et al (2006) PageMan: an interactive ontology tool to generate, display, and annotate overview graphs for profiling experiments. BMC Bioinformatics **7:** 535

Usadel B, Nagel A, Thimm O, Redestig H, Blaesing OE, Palacios-Rojas N, Selbig J, Hannemann J, Piques MC, Steinhauser D, et al (2005) Extension of the visualization tool MapMan to allow statistical analysis of arrays, display of corresponding genes, and comparison with known responses. Plant Physiol **138:** 1195–1204

Usadel B, Poree F, Nagel A, Lohse M, Czedik-Eysenberg A, Stitt M (2009) A guide to using MapMan to visualize and compare omics data in plants: a case study in the crop species, maize. Plant Cell Environ **32:** 1211–1229

Vicente AR, Saladié M, Rose JKC, Labavitch JM (2007) The linkage between cell wall metabolism and the ripening-associated softening of fruits: looking to the future. J Sci Food Agric **87:** 1435–1448

Vrebalov J, Ruezinsky D, Padmanabhan V, White R, Medrano D, Drake R, Schuch W, Giovannoni J (2002) A MADS-box gene necessary for fruit ripening at the tomato ripening-inhibitor (rin) locus. Science **296:** 343–346

Vriezen WH, Feron R, Maretto F, Keijman J, Mariani C (2008) Changes in tomato ovary transcriptome demonstrate complex hormonal regulation of fruit set. New Phytol **177:** 60–76

Wang H, Schauer N, Usadel B, Frasse P, Zouine M, Hernould M, Latché A, Pech JC, Fernie AR, Bouzayen M (2009) Regulatory features underlying pollination-dependent and -independent tomato fruit set revealed by transcript and primary metabolite profiling. Plant Cell **21:** 1428–1452

Wilkinson JQ, Lanahan MB, Yen HC, Giovannoni JJ, Klee HJ (1995) An ethylene-inducible component of signal transduction encoded by never-ripe. Science **270:** 1807–1809

Wise S, Reidegeld KA, Meyer HE, Warscheid B (2007) Protein labeling by iTRAQ: a new tool for quantitative mass spectrometry in proteome research. Proteomics **7:** 340–350

Yang S, Hoffman N (1984) Ethylene biosynthesis and its regulation in higher plants. Annu Rev Plant Physiol **35:** 155–189

Yang Y, Wu Y, Pirrello J, Regad F, Bouzayen M, Deng W, Li Z (2010) Silencing Sl-EBF1 and Sl-EBF2 expression causes constitutive ethylene response phenotype, accelerated plant senescence, and fruit ripening in tomato. J Exp Bot **61:** 697–708

Yang YH, Dudoit S, Luu P, Lin DM, Peng V, Ngai J, Speed TP (2002) Normalization for cDNA microarray data: a robust composite method addressing single and multiple slide systematic variation. Nucleic Acids Res **30:** e15

Yen HC, Lee S, Tanksley SD, Lanahan MB, Klee HJ, Giovannoni JJ (1995) The tomato Never-ripe locus regulates ethylene-inducible gene expression and is linked to a homolog of the Arabidopsis ETR1 gene. Plant Physiol **107:** 1343–1353

Zamboni A, Di Carli M, Guzzo F, Stocchero M, Zenoni S, Ferrarini A, Tononi P, Toffali K, Desiderio A, Lilley KS, et al (2010) Identification of putative stage-specific grapevine berry biomarkers and omics data integration into networks. Plant Physiol **154:** 1439–1459

Zarkovic J, Anderson SL, Rhoads DM (2005) A reporter gene system used to study developmental expression of alternative oxidase and isolate mitochondrial retrograde regulation mutants in Arabidopsis. Plant Mol Biol **57:** 871–888

Zhang J, Wang X, Yu O, Tang J, Gu X, Wan X, Fang C (2011) Metabolic profiling of strawberry (Fragaria x ananassa Duch.) during fruit development and maturation. J Exp Bot **62:** 1103–1118

Zhong S, Lin Z, Grierson D (2008) Tomato ethylene receptor-CTR interactions: visualization of NEVER-RIPE interactions with multiple CTRs at the endoplasmic reticulum. J Exp Bot **59:** 965–972